REVIEW

Check for updates

A review of zeolitic imidazolate frameworks (ZIFs) as electrochemical sensors for important small biomolecules in human body fluids

Zhou Feng,[a] H. N. Lim, [iD] *[ab] I. Ibrahim[bc] and N. S. K. Gowthaman [iD] [d]

Small biomolecules play a critical role in the fundamental processes that sustain life and are essential for the proper functioning of the human body. The detection of small biomolecules has garnered significant interest in various fields, including disease diagnosis and medicine. Electrochemical techniques are commonly employed in the detection of critical biomolecules through the principle of redox reactions. It is also a very convenient, cheap, simple, fast, and accurate measurement method in analytical chemistry. Zeolitic imidazolate frameworks (ZIFs) are a unique type of metal–organic framework (MOF) composed of porous crystals with extended three-dimensional structures. These frameworks are made up of metal ions and imidazolate linkers, which form a highly porous and stable structure. In addition to their many advantages in other applications, ZIFs have emerged as promising candidates for electrochemical sensors. Their large surface area, pore diameter, and stability make them ideal for use in sensing applications, particularly in the detection of small molecules and ions. This review summarizes the critical role of small biomolecules in the human body, the standard features of electrochemical analysis, and the utilization of various types of ZIF materials (including carbon composites, metal-based composites, ZIF polymer materials, and ZIF-derived materials) for the detection of important small biomolecules in human body fluids. Lastly, we provide an overview of the current status, challenges, and future outlook for research on ZIF materials.

[a] *Department of Chemistry, Faculty of Science, University Putra Malaysia, 43400 UPM Serdang, Selangor, Malaysia. E-mail: hongngee@upm.edu.my*

[b] *Foundry of Reticular Materials for Sustainability (FORMS) Laboratory, Institute of Advanced Technology, Universiti Putra Malaysia, 43400 UPM Serdang, Selangor, Malaysia*

[c] *Functional Nanotechnology Devices Laboratory (FNDL), Institute of Nanoscience and Nanotechnology, Universiti Putra Malaysia, 43400 Serdang, Selangor, Malaysia*

[d] *School of Engineering, Monash University Malaysia, Jalan Lagoon Selatan, 47500, Bandar Sunway, Selangor, Malaysia*

1. Introduction

Metal–organic frameworks (MOFs) are a relatively recent class of multifunctional micro-porous materials that have gained significant attention since their discovery in 1999. MOFs are composed of metal ions or clusters that are coordinated to organic ligands, forming one-, two-, or three-dimensional structures.[1–3] MOFs possess numerous advantages and unique

Zhou Feng is a PhD student at the Department of Chemistry, Faculty of Science, University Putra Malaysia (UPM). She joined Prof. Dr Hong Ngee Lim's research group in 2020 to pursue her doctoral studies. Her research focuses on developing electrochemical sensors for medical analysis at the graphene lab. Zhou is dedicated to fulfilling the requirements of her PhD degree and is committed to making significant contributions to the field of electrochemical sensors.

Zhou Feng

H. N Lim received her BSc and MSc degrees from Universiti Kebangsaan Malaysia. She was awarded a PhD degree in chemistry from Universiti Putra Malaysia. She is a Professor at the Department of Chemistry at University Putra Malaysia. Since 2009, she has been actively involved in graphene-related research, encompassing the synthesis of graphene-based nanomaterials and their applications.

H. N. Lim

This journal is © The Royal Society of Chemistry 2023

J. Mater. Chem. B, 2023, 11, 9099–9127 | 9099

properties, such as extensive surface areas, controllable morphology and pore sizes, varied structures, and unsaturated coordination sites.[2,4,5] Zeolitic imidazolate frameworks (ZIFs) are a well-known branch of the MOFs family that are composed of inorganic metal nodes connected by imidazole ester bridges or imidazole ligands. These porous hybrid materials exhibit excellent properties, including high thermal and chemical stability, tunable pore sizes, and exceptional gas separation and storage capacities.[6,7] Moreover, compared to many other MOFs, ZIFs exhibit remarkable properties that make them highly attractive for a wide range of applications, such as ultra-high surface areas, increased micropore volume, inherently low bulk density, various controllable pore geometry, and sizes, plenty accessible metal sites, varied topological structure and easily performed electrostatic interactions with different grafting functional groups.[6,8,9] In addition, ZIFs have attracted widespread attention and have undergone explosive development in various fields, including gas storage and separation, catalysis, drug delivery, chemo-sensors, luminescence, colorimetric sensing, surface-enhanced Raman scattering (SERS)-based sensing, and biomedicine.[8–10] In addition to their numerous applications in various fields, ZIFs and ZIF-derived materials have also been extensively studied for their potential use in electrochemical sensing applications. ZIFs offer several advantages in the design of electrochemical sensors. Their molecular-level channels enable the transport of small molecules and the doping of nanoparticles or molecules to create composites that enhance conductivity, among other properties. Moreover, ZIFs can serve as promising precursors that can be readily functionalized with active materials to generate porous nanocarbon composites that exhibit enhanced electrochemical performance.[8,10] Out of all the ZIF materials, ZIF-8, and ZIF-67, as well as their derivatives, are commonly employed as electrochemical sensors for detecting important small biomolecules in human body fluids. ZIF-8 (Zn-based) is composed of zinc

nitrate and 2-methylimidazole and is known for its stable skeleton and uniform internal pore size.[11,12] In contrast, ZIF-67 (Co-based) is made up of cobalt nitrate and 2-methylimidazole, and is characterized by its large surface area, high porosity, and biocompatibility.[10,13]

Biomolecules, including carbohydrates, proteins, lipids, and nucleic acids, are organic molecules that are produced by living organisms.[14,15] Human body fluids contain many types of important small biomolecules, such as dopamine (DA), uric acid (UA), ascorbic acid (AA), glucose, amino acids, and adrenaline.[16–18] The detection and analysis of these small biomolecules is of great importance in the field of clinical diagnostics and treatment, as it provides valuable information on their electrochemical reactions and allows for the quantification of their concentrations in human body fluids.[17] DA is often found alongside other molecular substances such as AA and UA in biological fluids within the human body.[19] As a result, many researchers have focused on developing methods for the simultaneous detection of AA, UA, and DA using voltammetry measurements. Studies have shown that DA exhibits oxidation/reduction peaks at voltage potentials similar to those of UA and AA on conventional solid-state electrodes. This can make it challenging to use traditional electrodes for the individual and simultaneous detection of these biomolecules, as electrode contamination and overlapping voltammetric responses can occur.[19–21] To address these challenges, there is a need for electrode materials with much higher electrocatalytic activity for the simultaneous detection of DA, AA, and UA, thus providing an electrochemical sensor with good selectivity, high sensitivity, and greater stability, simplicity, and convenience compared to other commercial detectors.[21–23]

It has been known that there are many different methods for the determination of small biomolecules, such as electrochemical methods,[13,16,17,24] capillary electrophoresis,[25–28] high performance liquid chromatography (HPLC),[29–32] fluorimetry,[33–38]

I. Ibrahim received his PhD degree in Materials Science from Universiti Putra Malaysia under the supervision of Prof. H. N. Lim in 2019. She is a postdoctoral fellow at the Institute Nanoscience and Nanotechnology (ION2) Universiti Putra Malaysia from 2019 till now. Her current scientific interests are carbon, metal–organic frameworks (MOFs), molecular-imprinted polymers (MIPs), and advanced nanomaterials for electroanalysis, energy storage, energy conversion, chemical sensor, photoelectrochemistry and water treatment research.

I. Ibrahim

N. S. K. Gowthaman is working as a Post-Doctoral Researcher at the School of Engineering, Monash University, Malaysia. He received his MSc degree from The Gandhigram Rural Institute, Tamil Nadu. He received his PhD degree under the supervision of Prof. S. Abraham John in the Department of Chemistry, The Gandhigram Rural Institute-Deemed to be University in 2017. His research interests are the fabrication of bimetallic nanoparticles and nanostructures and carbon nanomaterials/metal nanoparticles composite on electrode surfaces for the electrochemical sensing of environmental hazards and biomolecules and energy storage applications and he has published 56 research articles in it.

N. S. K. Gowthaman

9100 | J. Mater. Chem. B, 2023, 11, 9099–9127

This journal is © The Royal Society of Chemistry 2023

chemiluminescence,[39–44] colorimetry,[45–49] and optical sensing.[50–55] Electrochemical detection is a straightforward and convenient technique for detecting various biomolecules in human body fluids, and it has attracted growing interest unlike other methods.[56] So far, electrochemical sensors have been rapidly and continuously developed to detect various analytes by combining different electrochemical technologies with aptamer-based signal conversion strategies.[57] As reported, several well-known electrochemical analysis techniques have been proposed for the selective determination of small biomolecules, including cyclic voltammetry (CV), differential pulse voltammetry (DPV), chronoamperometry (CA), and square wave voltammetry (SWV).[1,8,57,58]

This article presents a review of the medical research and biological detection of biomolecules using ZIFs materials as electrochemical sensor electrodes in human body fluids. Firstly, the review discusses the synthesis methods of ZIFs for electrode fabrication, including various reaction parameters that may affect the electrochemical performance when detecting small biomolecules. Additionally, the electrochemical processes of ZIFs are discussed in detail, including how parameters such as scan rate, electrode type and area, electrolyte types, and ZIF material types can impact the performance of ZIF-based electrodes for the detection of different target analytes, with a focus on ensuring quality assurance. In addition, this review explores enzymatic and non-enzymatic electrochemical sensing techniques for evaluating the electrochemical abilities of ZIFs against various small biomolecules. The article aims to summarize the medical research and biological detection of biomolecules in human body fluids using ZIFs materials as electrochemical sensor electrodes. The synthesis methods of ZIFs for electrode fabrication are discussed, along with the electrochemical process of ZIFs and how various parameters can affect outcomes against different target analytes. Enzymatic and non-enzymatic electrochemical sensing techniques are explored, and detection methods for small biomolecules in actual samples using modified electrodes made of ZIF materials are also summarized. The proposed electrochemical sensors with modified ZIF electrodes have real application potential and can provide a reasonable recovery rate in actual samples.[6,13,59]

2. Importance of small biomolecules in the human body

Biomolecules are fundamental organic compounds with basic structural units that occur naturally in living cells or organisms and play a critical role in initiating and carrying out essential biochemical reactions in the human body.[14,15] DA, UA, AA, glucose, amino acids, and epinephrine are among the small biomolecules that are crucial components found in human body fluids, particularly in blood and urine. These biomolecules play a vital role in several physiological activities and are considered promising candidates for various applications.[23,60]

DA is considered the most significant and representative candidate among the small biomolecules as a neurotransmitter due to its crucial role in the central nervous, cardiovascular, renal, and hormonal systems of mammals and humans. As a result, it has garnered significant attention in the scientific community.[3,16] Low levels of DA have been linked to various neurological disorders and may result in pathological conditions such as Parkinson's disease, schizophrenia, Tourette's syndrome, HIV infection, cancer, and hyperprolactinemia.[19,21,61] Furthermore, UA is an important end-product of metabolism and is excreted in urine.[20] Abnormal levels of UA can lead to various disorders, including gout, hyperuricemia, Lesch-Nyan disease, and pneumonia.[21,62] AA is a crucial and ubiquitous nutrient that is essential for various biochemical and physiological processes. It plays a critical role in numerous biological activities, including cell division, gene expression, and the activation of natural defense mechanisms.[63–65] Severe AA deficiency can lead to adverse symptoms such as weak joints, bleeding gums, and skin discoloration caused by ruptured blood vessels.[66]

Glucose is a small and simple sugar that is a vital component of the human body. It plays a particularly crucial role in the metabolic process and serves as an energy source in living systems to support the proper functioning of humans.[67] Moreover, glucose has practical value in various fields, including medical applications such as blood glucose analysis, biotechnology, food industries, and environmental monitoring.[68,69] It is well known that uncontrolled glucose levels in human fluids such as serum, urine, and saliva can cause chronic hyperglycemia, which can lead to various diseases such as heart disease, blindness, kidney failure, hypertension, and cancer.[24,69,70] As a result, glucose sensors have gained significant attention and interest from many scientists due to their potential benefits.

Amino acids are essential for the survival, growth, development, reproduction, and overall health of all organisms, and they play multiple roles in human physiology.[71,72] Deficiencies in certain amino acids can lead to various diseases. For instance, a deficiency in tyrosine may induce depression, dementia, and hypothyroidism, while an elevation in tyrosine can cause Parkinson's disease and hyperthyroidism. Additionally, abnormal concentrations of tryptophan in the blood may lead to autism and schizophrenia.[6,13] Moreover, adrenaline is a critical component of the acute stress response system in the human body, and a low concentration of adrenaline can also lead to Parkinson's disease.[73] In other words, amino acids, and adrenaline, as neurotransmitters, are crucial components present in our human body fluids. Therefore, the following sections will discuss the electrochemical detection of small biomolecules in human body fluids using ZIFs or ZIFs-derived materials.

3. General aspects for electrochemical assays of small biomolecules using ZIFs

This section provides a summary of various electrochemical sensors fabricated from ZIFs and ZIF-derived materials, and their properties are presented in Tables 1–3. The tables show that most researchers aim to detect small biomolecules in human body fluids, such as DA, UA, AA, glucose, amino acid,

This journal is © The Royal Society of Chemistry 2023

J. Mater. Chem. B, 2023, 11, 9099–9127 | 9101

Table 1 Summary of sensors fabricated from ZIFs and ZIF-derived materials for detection of DA

SBs	Sensor	Modification	Method	Linear range (μM)	LOD (μM)	Sensitivity (μA mM^{-1} cm^{-2})	Simultaneous detection	Real sample	Ref.
DA	ZIF-8@Co-TA/CPE	DC	DPV	0.02–0.44	0.0034	—	UA, AP, Trp	Serum	6
	ZIF-8 derived N-CF@N, PCF/GCE	DC	DPV	0.05–7.5	0.0222	20 5400	UA, AP, HQ, catechol	Urine, serum	8
	ZIF-8 derived Nafion–NGR–NPC/GCE	DC	DPV	0.08–350	0.011	—	UA, AA	Urine	59
	DA-imprinted CS film/ZnONPs@C/3D-KSC/IE	ED	DPV	0.00012–152	0.000039	757	—	DA	74
	MIPs/CuCo$_2$O$_4$@carbon/3D-KSC/IE	ED	DPV	0.51–1950	0.16	720.8	—	—	75
	CoP@C/NCS/GCE	DC	CA	5.0–400	0.03	9.4 μA μM^{-1}	—	Serum	76
	HP-ZIF-8/3DCNTs/GCE	DC	DPV	0.1–100	0.027	—	—	—	77
	Ag-ZIF-67p/GCE	ED	DPV	0.1–100	0.05	—	AP	DA	78
	Au@ZIF-8/GCE	DC	DPV	0.1–50	0.01	93.7	—	—	79
	ZIF-67/rGO/GCE	DC	CA	0.25–1216.25	0.05	6.452	H$_2$O$_2$	—	80
	Ni-ZIF-8/N S-CNTs/CS/GCE	DC	DPV	8–500	0.93	—	UA, Trp	Urine, serum, amino acid	81
	ZIF-67/GCE	DC	DPV	2–22	1.3	—	PA	DA	82
	Pt41Rh59 alloy/ZIF-90/GCE	DC	CA	0.001–0.01, 0.025–5	0.001	2.14 A M^{-1} cm^{-2}	—	—	83
	ZIF-67 derived CN@Co/Pt/Co/GCE	ED	CA	0.002–1.04,	0.00276,	17 380	—	Living C$_6$ cells	84
			DPV	1–200	0.0213	2076			
	PPy/ZIF-67-MIPs/Nafion/GCE	DC	DPV	0.08–100, 100–500	0.0308	1656	—	DA, serum	85
	GO-ZIF-67/GCE	ED	DPV	0.2–80	0.05	1387	UA	Urine	86
	Co/CoN@NPC/CPE	DC	DPV, CA	0.01–50, 50–500	0.006	12 400 ± 300	—	Urine, DA	87
	Nafion/PANI/ZIF-8/GCE	DC	DPV	0.1–100	0.012	—	—	Serum	88
	NCCNPs800/GCE	DC	DPV	2–196.1	0.34	1.1303 μA μM^{-1}	UA	—	89
	RGO/ZIF-8/GCE	DC	DPV	0.1–100	0.03	0.1527 μA μM^{-1}	—	Serum	90
	ZIF8@ZnO@GO/GCE	ED	CA	0.0005–0.002		—	—	—	91
	ZIF-8/GCE	DC	DPV	0.05–20	0.195	—	—	—	92
	G-ZIF8/GCE	DC	CA	3–1000	1	0.34 μA μmol^{-1} L^{-1}	—	Cow serum	93
	Fe$_3$O$_4$@ZIF-8/RGO/GCE	DC	DPV	0.002–10	0.000667	—	—	Serum, urine	94
	ZIF-8 derived N-PCNPs O-/GCE	DC	DPV	0.5–30	0.011	—	UA, AA	Urine	95

ED = electrodeposition, DC = drop-coating; AP = Acetaminophen, HQ = hydroquinone, Trp = tryptophan.

and adrenaline, using ZIFs and ZIF-derived materials for electrochemical sensing applications. This article provides a summary of various electrochemical methods, and the most used detection techniques are CV, DPV, and amperometry (AMP) or chronoamperometry (CA), which exhibit high sensitivity and selectivity for small biomolecule detection using ZIFs and ZIF-derived materials. Among these sensors, the most used modification method is drop-coating, which involves modifying the surface of a glassy carbon electrode (GCE) with the ZIF or ZIF-derived materials for the electrochemical detection of small biomolecules. Electrochemical sensors with high sensitivity are fabricated using better electrode materials, such as ZIFs, which facilitate increased electron transfer and mass transfer, leading to improved sensing performance. Based on Table 1, it is evident that the majority of electrochemical sensors have LODs (limit of detection) below 1 μM, with the lowest LOD recorded as 0.039 nM for the DA-imprinted CS film/ZnONPs@C/3D-KSC integrated electrode (IE), which exhibited excellent catalytic activity for DA detection.[74] Furthermore, the electrochemical sensor for DA detection based on MIPs/CuCo$_2$O$_4$@carbon/3D-KSC integrated electrode exhibited the widest linear range of 0.51–1950 μM, covering a broad range of DA concentrations, while maintaining high sensitivity in electrode reactions.[75]

Table 1 shows that the majority of electrochemical sensors demonstrated excellent anti-interference ability and stability, and their application potential was confirmed by their outstanding recoveries in real samples such as serum, urine, and DA injection. Table 2 highlights that most of the electrochemical sensors have LODs below 1 μM, with the lowest recorded value of 7.35 nM achieved by gt-NiCo$_2$O$_4$ NSs/GCE for the detection of glucose (GLC), demonstrating its exceptional catalytic activity.[70] In addition, the GLC electrochemical sensors presented a much wider detection range compared to DA electrochemical sensors, and they exhibited good recoveries in real samples, with most of the samples being serum. In addition, as shown in Table 3, there are lesser ZIFs materials for detecting UA, AA, amino acid, and adrenaline, indicating that it is a good challenge for scientists can find much better ZIFs materials as electrochemical sensors, which can be applied to more fields in the future.

3.1 Synthesis methods of ZIFs for electrodes fabrication

In recent decades, there has been growing interest in the development of various synthesis methods for ZIFs. ZIFs are typically synthesized using solvothermal and hydrothermal methods. However, other synthesis methods have also been

9102 | J. Mater. Chem. B, 2023, 11, 9099–9127

This journal is © The Royal Society of Chemistry 2023

Table 2 Summary of sensors fabricated from ZIFs and ZIF-derived materials for detection of GLC

SBs	Sensor	Modification	Method	Linear range (µM)	LOD (µM)	Sensitivity (µA mM^{-1} cm^{-2})	Simultaneous detection	Real sample	Ref.
GLC	Co$_3$O$_4$/MWCNTs/Au/GCE	DC	CA	0.1–1100	0.1	1138.4	—	Sports drink	68
	rGO@Co$_3$O$_4$-NC/ITOE	DC	CA	0.5–20	0.0504	2563	—	Serum	69
	gt-NiCo$_2$O$_4$ NSs/GCE	DC	CA	0.15–8860	0.00735	729.72	—	Urine, serum	70
	NiCo NSs/GNR-GCE	DC	CA	5–800, 1–1000	0.6	344	—	Serum	96
	GC/MW/PB/ZIF-8@GOx	DC	CA	1000–10 000	50	—	—	Serum	97
	Co@NCD/GCE	DC	CA	0.2–1200	0.11	125	—	Serum	98
	Co$_3$O$_4$@CCCH NWs/CF	DC	CA	1–2000	0.48	16 010	—	Serum	99
	Ag@TiO$_2$@ZIF-67/GCE	DC	CA	48–1000	0.99	788	—	—	100
	CoFe-PBA/Co-ZIF/NF	DC	CA	1.4–1500	0.02	5270	—	Serum	101
	Cu@HHNs/GCE	DC	CA	5–3000	1.97	1594.2	—	Serum	102
	HierarchicalCo$_3$O$_4$/NiCo$_2$O$_4$/CCE	ED	CA	1–1127	0.64	0.012835	—	Serum	103
	NiCo$_2$O$_4$ HNCs/GCE	DC	CA	0.18–5100	0.027	1306	—	Serum	104
	ZIF-67derived Co$_3$O$_4$/NCNTs/GCE	DC	CA	5–2650, 4650–13 650	5	87.40	H$_2$O$_2$	—	105
	ZIF-67 derived CoP/Co-BP/SCE	DC	CA	0.5–1800	0.2	6427	—	Serum	106
	Au@NiCo LDH/GCE	DC	CA	5–12 000	0.028	864.7	—	—	107
	Cu-Co-ZIFs/GCE	DC	CA	20–800	2	0.01868	—	—	108
	Ni$_3$(PO$_4$)$_2$@ZIF-67/GCE	DC	CA	1–4000	0.7	2783	—	Serum	109
	CoO-Co-NC-rGO/GCE	DC	CA	0.5–10	0.34	3172	—	Serum	110
	GS@ZIF-67/GCE	DC	CA	1–805.5	0.36	1521.1	—	Serum	111
	Gox@ZIF-8 (TiO$_2$)/GCE	DC	CA		0.08	—	—	Sweat, saliva	112
	GOx/Fe$_3$O$_4$/PPy@ZIF-8/GCE	DC	CA	1–2000	0.33	—	—	Serum	113
	Gox@ZIF-8(AuNPs)/GCE	DC	CA		0.05	—	—	Sweat/saliva	114
	Ni/NPC/GCE	DC	CA	1–7940	0.3	3753.78	—	Serum	115
	Ag@ZIF-67/GCE	DC	CA	2–1000	0.66	379	—	—	116
	GOx-CHIT/Co$_3$O$_4$ NPs/Au	DC	CA		0.1	—	UA	Tears	117
	GOx/H-ZDPC/SPCE	DC	CA	500–2900, 3850–14 500	141.6	10.86, 3.65	—	—	118
	Co$_3$O$_4$/NiCo$_2$O$_4$ DSNCs@G/GCE	DC	CA	10–3520	0.384	0.000196	—	Serum	119
	Co$_3$O$_4$-HND/GCE	DC	CA	2–6060	0.58	708.4	—	—	120
	Cu-in-ZIF-8/SPCE	DC	CA	0–700	2.76	0.000412	—	Rat serum	121
	GOx/PDA/ZIF-8@rGO/GCE	DC	CA	1–1200, 1200–3600	0.333	—	—	Serum	122
	Ag@ZIF-67/MWCNT/GCE	DC	CA	33–400	0.49	13 014	—	Serum	123
	ST-Co3O4/CCE	DC	CA	1–1300	0.19	2860	—	Serum	124
	ZIF-67 HNPs/GCE	DC	CA	5–3300, 3300–42 100	0.96	445.7	—	Serum	125

derived from these, such as son-chemical, mechanochemical, and ion-thermal synthesis.[9] The synthesis of ZIF-8 in high purity can be achieved using various routes, with solvothermal synthesis being one of the most common and environmentally friendly methods.[12] The typical synthesis method of ZIF-8 involves a solvothermal process at room temperature for a short duration, using zinc nitrate hexahydrate and 2-methylimidazole, as shown in Fig. 1a.

ZIF-8 can be synthesized by various methods, including solvothermal, microwave-assisted, son-chemical, mechano-chemical, dry-gel conversion (DGC), microfluidic, and electro-chemical methods.[12] It can be observed from Fig. 1b that all the ZIF-8 samples synthesized using different methods have uniform crystal facets, with particle sizes ranging from 200 nm to 2 µm. Additionally, the BET surface area of the ZIF-8 samples range from 1249 to 1580 m^2 g^{-1}, indicating that ZIF-8 has high porosity and a large surface area.[12] From Fig. 1b, it can be observed that all these ZIF-8 samples have well-defined hexagonal morphologies, except for ZIF-8 synthesized by the electrochemical method, which had irregular shapes. The particle size also varies due to the different synthesis methods; for example, ZIF-8 synthesized using dimethylformamide (DMF) solution produced the largest particle size of ZIF-8

(150–200 µm).[8] When using sono-chemical and DGC methods, ZIF-8 had the smallest particle size, between 0.3–0.5 µm. It is known that he smaller the size of the particle, the larger its surface area. Therefore, ZIF-8 synthesize via the sono-chemical and DGC methods provides a larger surface area which is beneficial to be introduced in electrochemical sensors.

The synthesis route for ZIF-67 shown in Fig. 1c is the solvothermal method at room temperature with a synthesis duration of 6 hours, using cobalt nitrate and 2-methy-limidazole. This method is widely used and similar to the synthesis of ZIF-8.[10,138] Another work utilized the hydrothermal method to synthesize ZIF-67 nanocrystals with a particle size ranging from 78 to 385 nm (average size = 228 nm) and a surface area of 316 m^2 g^{-1}. It was reported that the average particle sizes could be increased from 689 nm to 5.2 µm when the concentration of pure aqueous solutions was decreased.[139] The small particle size and larger surface area of ZIF-67 make it a promising material for various electrochemical sensor applications.

The microwave-assisted method was used to synthesize pure ZIF-67 nanocomposite, which showed excellent electron transfer efficiency, good electrocatalytic activity, and high adsorption capacity.[82] The previously mentioned electrochemical sensor

This journal is © The Royal Society of Chemistry 2023

J. Mater. Chem. B, 2023, 11, 9099–9127 | 9103

Table 3 Summary of sensors fabricated from ZIFs and ZIF-derived materials for detection of UA, AA, amino acid, and adrenaline

| SBs	Sensor	Modification	Method	Linear range (µM)	LOD (µM)	Sensitivity (µA mM^{-1} cm^{-2})	Simultaneous detection	Real sample	Ref.
UA	ZIF-8@Co-TA/CPE	DC	DPV	0.02–0.44	0.0012	—	DA, AP, Trp	Serum	6
	ZIF-8 derived N-CF@N, PCF/GCE	DC	DPV		0.0245	20 5000	DA, AP, HQ, catechol	Urine, serum	8
	ZIF-8 derived Nafion–NGR–NPC/GCE	DC	DPV	0.5–100	0.088	—	DA, AA	Urine	59
	Ni-ZIF-8/N S-CNTs/CS/GCE	DC	DPV	1–600	0.41	—	DA, Trp	Urine, serum, amino acid	81
	GO-ZIF-67/GCE	ED	DPV	0.8–200	0.1	482	DA	Urine	86
	NCCNPs800/GCE	DC	DPV	5–370.4	0.98	610.7 µA mM^{-1}	DA	—	89
	ZIF-8 derived N-PCNPs/GCE	DC	DPV	4–50	0.021	—	DA, AA	Urine	95
	GOx-CHIT/Co$_3$O$_4$ NPs/Au and BSA CHIT/Co$_3$O$_4$/Au	DC	CA		0.1	—	GLC	Tears	117
	Z-11/GCE	DC	DPV	20–540	0.48	174	—	Urine	126
	Au/Co@HNCF	DC	DPV	0.1–25, 25–2500	0.023	48 400	—	Serum	127
	ZIF-67/g-C$_3$N$_4$/GCE	DC	DPV	0.2–6.5	0.052	—	AP	Urine	128
	CNCo/GCE	DC	DPV	2–110	0.83	—	—	Serum	129
	Z-1000/GCE	DC	DPV	1–300	0.014	—	Catechol, HQ	Serum	130
AA	ZIF-8/Pt NPs/GCE	ED	DPV	10–2500	5.2	959.9	—	Serum	131
	MIPs/ZIF-67/CCE	ED	CA	0.057–11 400	0.019	—	—	Serum	132
	ZIF-65@ CNTs electrode	DC	DPV	200–2267	1.03	—	—	—	133
	Fc (COOH)2/ZIF-8/3D-KSCs	ED	CV	0.06–5010	0.017	—	—	—	134
Trp	ZIF-8@Co-TA/CPE	DC	DPV	0.02–0.44	0.0067	—	UA, AP, DA	Serum	6
	Ni-ZIF-8/N S-CNTs/CS/GCE	DC	DPV	5–850	0.69	—	DA, UA	Urine, serum, amino acid	81
	PDMS@cZIF/GCE	DC	DPV	0.5–72	0.17	—	Adrenaline, serotonin	Rat blood samples	135
Cys	Co$_3$O$_4$-NPCN@GCE	DC	CA	0.05–5200	0.0069	63.4	—	Serum	136
Tyr	MIP/pTH/Au@ZIF-67/GCE	DC	DPV	0.01–4	0.00079	—	—	Serum	13
Adrenaline	PDMS@cZIF/GCE	DC	DPV	0.3–65	0.09	—	Trp, serotonin	Rat blood samples	135
	ZIF-67/NC/3DG Fiber electrode	ED	CV	0.06–95 95–5900	0.02	0.011	—	Serum	137

Tyr = tyrosine, Cys = L-cysteine.

for the detection of DA and paracetamol has been reported to have high sensitivity, a low detection limit, and good reproducibility. Another study reported the rapid synthesis of pure ZIF-8 nanocrystals *via* the ultrasonic-assisted solvothermal method for the electrochemical detection of DA. It was found to be a suitable candidate for excellent electrode materials and demonstrated good anti-interference ability and long-term stability as an electrochemical sensor.[92] The results indicate that the distinct electrochemical reaction of pure ZIF-8 or ZIF-67 to DA molecules is due to their planar geometric structure and particular pore property. Additionally, these two types of sensors detected DA linearly over a smaller concentration range with a lower detection limit compared to other ZIFs sensors. However, more sensitive ZIFs sensors can be developed by incorporating electrically conductive components such as carbon, polymers, or metal nanoparticles, to create new nanocomposites with improved electrical conductivity compared to pure ZIF materials.

There are two types of deposition methods commonly used for the preparation of ZIF materials electrodes for the detection of small biomolecules in human body fluids: drop-coating (DC) and electrochemical deposition (ED). The drop-coating method is considered the most useful and general method for preparing modified electrodes with ZIFs materials. This method involves the formation of a thin solid film by dropping a solution containing ZIFs onto the electrode surface, followed by evaporation of the solvent at room temperature. The drop-coating method is a simple, convenient, and fast technique that is widely used to prepare modified electrodes. The modifying layer is composed of nanocomposites, which enables a uniform distribution of these nanoparticles across the electrode area and is commonly applied in electrocatalytic analysis and electrochemical sensing.[140] The most used electrodes in electrochemical sensors are typically graphene-modified glassy carbon electrode (GCE), screen-printed carbon electrode (SPCE), and carbon paste electrode (CPE). The GCE is a widely used carbon electrode material in electrochemistry due to its many advantages, such as its exceptionally smooth and homogeneous surface, ease of polishing and reusability, low cost, small test area and high sensitivity, resistance to interference, larger

9104 | J. Mater. Chem. B, 2023, 11, 9099–9127

This journal is © The Royal Society of Chemistry 2023
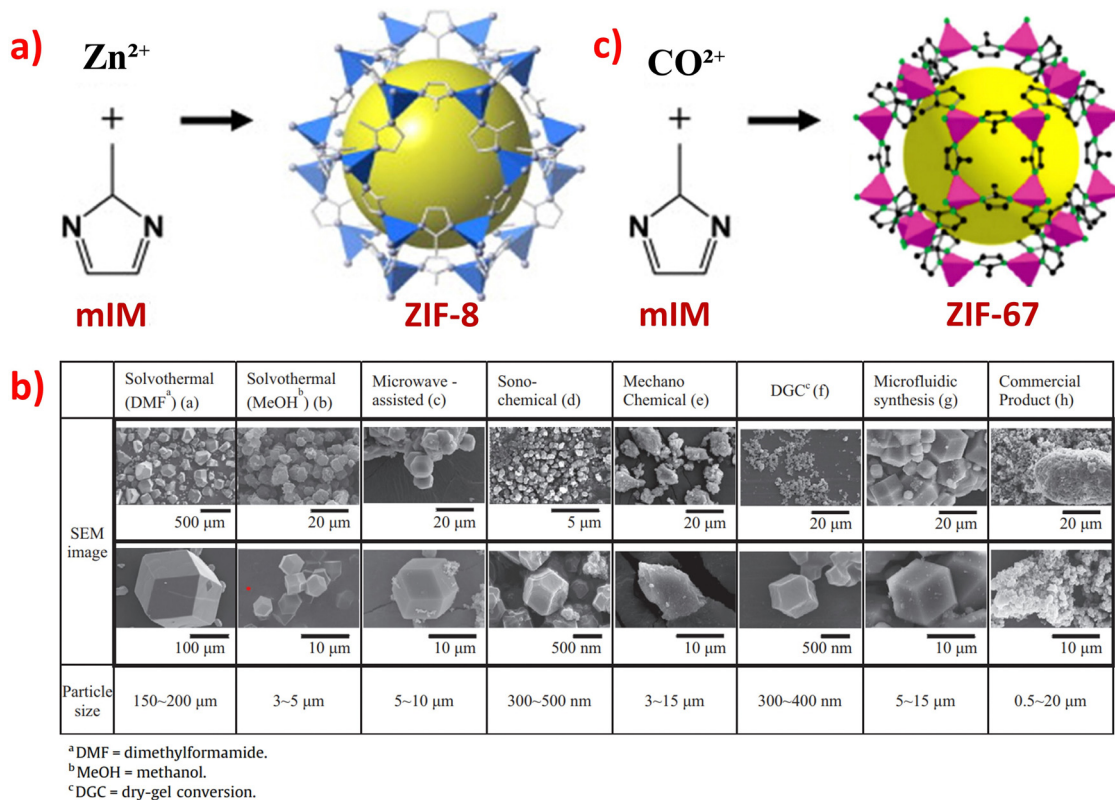
Fig. 1   (a) Crystal structure synthesis route of ZIF-8. (b) SEM images of the ZIF-8 samples prepared using different synthesis methods. Reproduced with permission from ref. 12. Copyright (2015) Elsevier. (c) Crystal structure synthesis route of ZIF-67. Reproduced with permission from ref. 138. Copyright (2009) ACS.

electrochemical window, as well as impressive mechanical properties and chemical resistance. However, it has slow electron transfer kinetics.[141] Additionally, Nafion (NF) is an excellent binder to modify the GCE of ZIFs materials. Also, the negatively charged hydrophilic sulfonate groups in the NF polymer structure help accumulate the positively charged molecules *via* electrostatic interaction, resulting in enhanced sensitivity of the measurements.[142] Compared to the drop-casting method, the electrodeposition method offers more stability and better electrochemical performance for detecting important small biomolecules in human body fluids.[86] The modified electrodeposition method has been shown to significantly enhance the electrocatalytic performance of ZIFs nanocomposites. Electrodeposition is a fascinating phenomenon and a flexible, low-cost method of fabricating ZIFs materials. It is a suitable method for modifying electrode surfaces in nanoscience and nanotechnology, as it can produce excellent effects on the characteristics and functionalities of ZIFs materials at the nanoscale level.[143]

3.2   Electrochemical detection methods using ZIFs as electrode materials

Conventional techniques in analytical chemistry, such as spectroscopy and chromatography, rely on distinct principles for analysis, which involve optical or physical measurements.[144,145] Unlike conventional techniques, the electrochemical method is a common

analytical technique that uses a measurement of charge, potential or current to investigate or evaluate the relationship between the analyte's concentration and its chemical reactivity. The use of electrochemical sensors for the detection of biomarkers in body fluids displays promising diagnostic technologies and can be applied to various fields.[146,147] Therefore, electrochemical sensors or biosensors can be defined as analytical devices that convert the information of the oxidation/reduction reaction between the electrode and target molecules into a measurable electronic output signal in response to a biological or chemical analyte. A simple electrochemical sensor system consists of three components: the sample analyte, the transducer, and the measurable signal.[22] There are three main types of electrochemical techniques that can be used in sensors for the detection of important small biomolecules in body fluids: voltammetric, amperometric, and potentiometric methods.[147] Voltammetric sensors are modified-electrode-based sensor systems widely used in various fields, for instance, inorganic, physical, and biological sciences. Furthermore, voltammetric sensor systems can be applied in various types of sensors, and many of them are based on GCE modified with ZIFs materials that enable rapid and accurate detection of important small biomolecules.[148] Different voltammetric techniques can be distinguished by the modes of the applied potential to the working electrode and the type of ZIF material used as the working electrode modifier. These techniques can be described as follows: cyclic voltammetry (CV), differential pulse voltammetry (DPV),

electrochemical impedance spectroscopy (EIS), chronoamperometry (CA), and square wave voltammetry (SWV).[6,17,57,58] CV and DPV are common electrochemical detection methods used to measure the current response of redox reactions. These methods can quickly determine response signals related to the thermodynamics of redox processes, the energy levels of the analyte, and the kinetics of electronic transfer reactions. In addition, the electrochemical properties of important small biomolecules can be analyzed, and the selectivity, reproducibility, repeatability, and stability of ZIFs-based electrochemical sensors can be investigated. Use right sentence.[22,77,149] Mainly, they can be utilized for the simultaneous determination of DA, AA, and UA with activation overpotentials.[149] The EIS technique can be used to investigate the capability of ZIF-modified electrodes to transfer and convert electric charge with target molecules, and to obtain impedance signals from the modified electrodes.[17] Chronoamperometry is a technique in which the potential of a working electrode is held constant, and the resulting current is measured as a function of time. This method is often used to determine the concentration of a specific species in a solution, and its sensitivity and selectivity can be affected by the choice of electrode material, solution composition, and experimental conditions.[150–152] In addition, SWV is a powerful electrochemical technique that effectively separates faradaic processes from charging currents by applying a series of square-shaped potential pulses on top of a staircase potential sweep.[153]

An amperometry sensor system is a type of electrochemical sensor that measures the current produced by a chemical reaction in the analyte at a fixed potential, often using a reference electrode. The voltage applied between two electrodes during amperometric measurement can be utilized in various fields, including biology, medicine, industry, energy production, safety, health, defense, sport, environment, and agriculture. Amperometric electrochemical sensing was initially developed in the 1970s as an amperometric detector in the analytical system.[154,155] Amperometric techniques have been widely used to determine glucose levels and are commonly employed in small, minimally invasive devices such as glucose meters for diabetes management.[156] Potentiometric sensors usually measure the potential difference between two electrodes in the absence of current flow. This sensor has been widely used in ion-selective electrodes (ISEs) and ion-selective field-effect transistors (ISFETs) for physiological testing of primary electrolytes. Potentiometric sensors measure the potential change of one electrode relative to a reference electrode or a ground electrode in the absence of current flow.[156,157] Additionally, the potentiometric technique has been routinely used for physiological testing and can measure different substances like some ions or other small biomolecules.[158]

3.3 Enzymatic and non-enzymatic electrochemical sensors based on ZIFs

The rapid, sensitive, and accurate detection of important small biomolecules using enzymatic and non-enzymatic electrochemical sensing techniques has attracted enormous interest due to fast developments in medical science and technology fields.[119,122] Enzyme-based electrochemical sensors are constructed by immobilizing enzymes on the substrate materials to create a high-performance bio-electrocatalytic system based on biological recognition. These sensors adjust the enzyme orientation on conductive vehicles, allowing for the transfer of electrons between active sites of enzymes and electrodes to catalyze a specific biochemical reaction.[118,127] It has been reported that some biosensors use oxidase enzymes to catalyze the reaction between the analyte and oxygen as a natural electron acceptor, producing detectable molecules.[141] The development of high-performance electrochemical enzymatic sensors requires substrate materials with a large surface area and good conductivity. Some ZIFs materials have been shown to meet these requirements and are used in the fabrication of such sensors.[118] Enzyme-based electrochemical sensing devices have many advantages, such as increasing electrochemical communication, high sensitivity, and high selectivity.[97] However, these biosensors also have some intrinsic disadvantages, such as higher fabrication cost than non-enzymatic biosensors, sensitive to environmental factors, low stability, poor reproducibility, and complicated modification procedure.[24,141] The immobilization of electrocatalysts and dehydrogenase on the surface of the electrode using ZIFs as a matrix has facilitated the development of integrated electrochemical biosensors for glucose detection *via* enzymatic electrocatalysis.[10] Enzymatic electrochemical glucose sensors typically utilize glucose oxidase (GOx) or glucose dehydrogenase (GDH).[24] Other small biomolecules mostly use non-enzymatic electrochemical sensors based on ZIFs materials.

Non-enzymatic electrochemical sensors are considered as promising analytical devices due to their essential advantage of enzymatic invariance, which has attracted significant attention from scientists. The key is that the electrode materials are based on nonenzymatic material, which can catalyze and promote the electrochemical reaction. Therefore, exploring electrode materials based on ZIFs is considered an important research direction and challenge in the field of electrochemistry.[69] In recent years, many scientists have devoted significant effort to developing various electrode materials based on ZIFs for use in non-enzymatic detection.[24] An example of this is the development of a novel electrochemical sensor that utilizes porous carbon derived from bimetallic ZIFs, which has demonstrated good analytical performance and successfully detected UA in human serum samples.[129] Researchers have fabricated a new sensor for AA based on a ZIF-65@CNTs nanohybrid with a designable structure and high sensory performance.[133] A non-enzymatic glucose sensor was developed using a three-dimensional copper foam-based supporter decorated with Co_3O_4 hierarchical nanostructure, which exhibited high electrocatalytic properties for actual applications.[99] Compared with enzymatic sensors, non-enzymatic sensors have many advantages, such as being hardly affected by oxygen, having a simple manufacturing process, good thermal and chemical stability, low cost, good reproducibility, rapid response, excellent selectivity, high sensitivity and accuracy, continuous monitoring, and high throughput.[16,158]
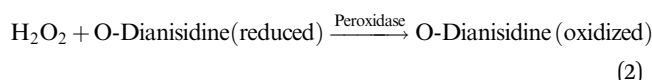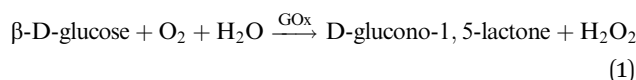
9106 | *J. Mater. Chem. B*, 2023, **11**, 9099–9127

This journal is © The Royal Society of Chemistry 2023

Most electrochemical sensors based on ZIFs are non-enzymatic devices that rely on direct oxidation.[24] On the one hand, a novel proof-of-concept DA molecular imprinting sensor based on Cu/Co-ZIF-derived $CuCo_2O_4$@porous carbon/3D-KSCs nanocomposites exhibited good stability and excellent anti-interference ability.[75] A composite material consisting of a DA-imprinted chitosan film/ZnONPs@carbon nanosphere/3D kenaf stem-derived microporous carbon nanocomposite was prepared, which exhibited better selectivity for DA detection.[74] However, the use of ZIFs for indirect non-enzymatic detection of small biomolecules is still rare. Additionally, designing and synthesizing cost-effective novel electrocatalytic sensors based on ZIF materials still face many difficulties and challenges in the future.

3.4 Reaction mechanism for electrochemical detection of small biomolecules using ZIFs

The reaction mechanism of enzymatic electrochemical sensors is complex. For example, an electrochemical UA biosensor was prepared using a modified hollow nonporous carbon framework with ultrafine gold/cobalt nanoparticles (Au/Co@HNCF) synthesized by the pyrolysis of an Au(III)-etching zeolitic imidazolate framework-67 (ZIF-67) as an enzyme to fabricate the electrode. The article reported that ZIF-67 includes imidazole rings with sp^2-conjugated bonds (π–π interaction), and that the π–π stacking interaction between the phenyl structures of UA and the three-dimensional imidazolate structure of ZIF-67/g-C_3N_4 makes it conducive for the imidazolate structure to adsorb on the surface of the modified electrode. The cooperation between the nitrogen atoms in the analytes and Co(II) ions adopted UA to the surface of the modified electrode, and the oxidation mechanism is proposed in Fig. 2.

There have been many ZIF@enzyme-based amperometric glucose sensing approaches, and the reaction mechanism is also intricate. Various enzymes have been used in these approaches, including glucose oxidase (GOx), organophosphate degrading enzyme A (OpdA), α-chymotrypsin, glucose dehydrogenase, tyrosinase, and others.[97] GOx is one of the most widely studied enzymes and is susceptible to pH and temperature. It catalyzes the reaction of β-D-glucose to gluconic acid, and the oxidation reaction results in the formation of hydrogen peroxide.[97,112] A good example utilizes GOx enzyme to catalyze the oxidation of glucose to yield hydrogen peroxide, which further oxidizes dianisidine in the presence of horseradish peroxidase, resulting in a colored product that is monitored at 460 nm. The reaction equations for this process are eqn (1) and (2).[97]

$$\beta\text{-D-glucose} + O_2 + H_2O \xrightarrow{\text{GOx}} \text{D-glucono-1,5-lactone} + H_2O_2 \tag{1}$$

$$H_2O_2 + \text{O-Dianisidine(reduced)} \xrightarrow{\text{Peroxidase}} \text{O-Dianisidine(oxidized)} \tag{2}$$

Another example involves the oxidation of glucose by GOx enzyme to generate gluconate and H_2O_2, which can be absorbed by 4-aminobenzophenone (chromogenic oxygen acceptor) and react with phenol to produce peroxidase quinone dye. The dye then turns red after the reaction. The reaction equations for this process are eqn (3) and (4).[112]
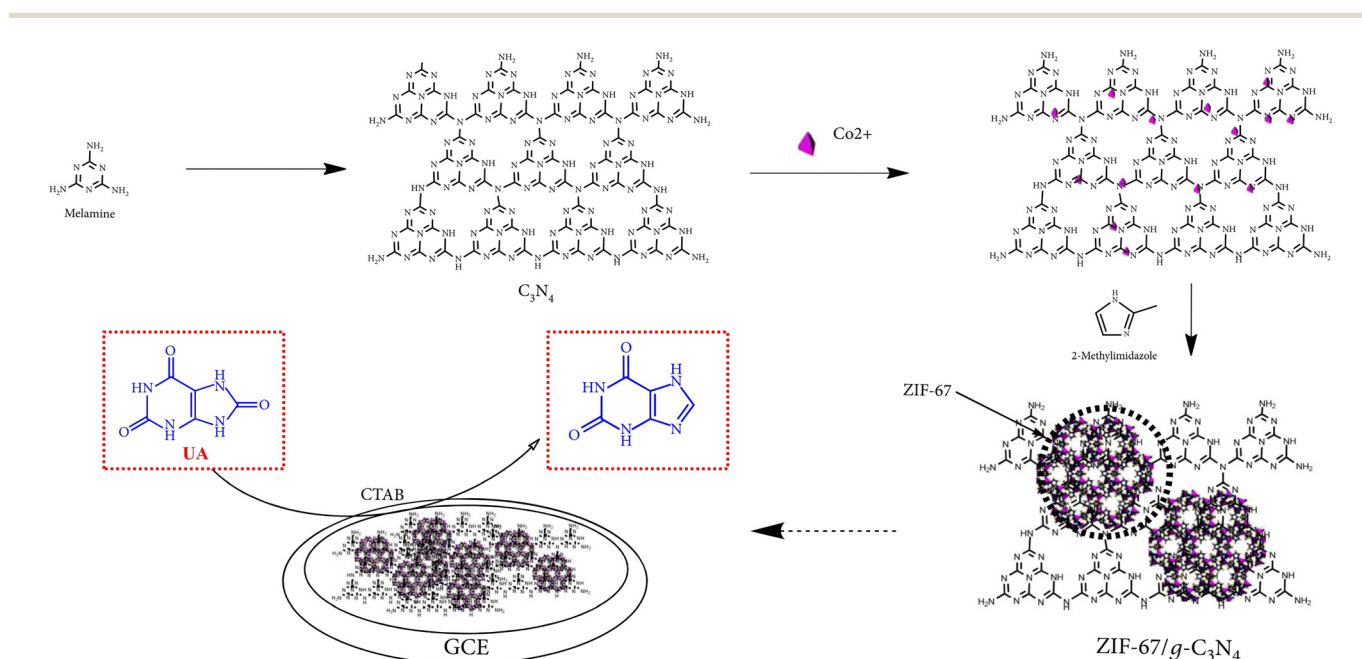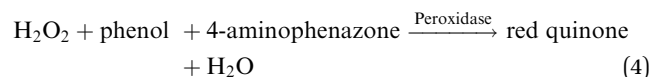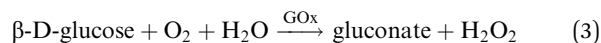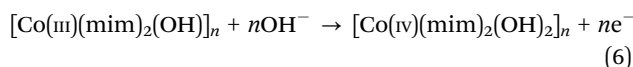
$$\beta\text{-D-glucose} + O_2 + H_2O \xrightarrow{\text{GOx}} \text{gluconate} + H_2O_2 \tag{3}$$

$$H_2O_2 + \text{phenol} + \text{4-aminophenazone} \xrightarrow{\text{Peroxidase}} \text{red quinone} + H_2O \tag{4}$$

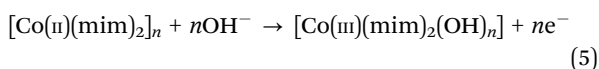Fig. 2 Reaction mechanism of UA oxidation at the ZIF-67/g-C_3N_4-modified electrode. Reproduced with permission from ref. 128. Copyright (2020) Hindawi.

Two papers utilized the GOx enzyme to catalyze the oxidation of glucose-to-glucose acid and H_2O_2; once H_2O_2 flowed out, the peroxidase-like ZIFs nanocomposites outside the electrode catalyzed H_2O_2 to H_2O, causing the simultaneous receiving and losing of electrons.[113,122] Their mechanism is shown in Fig. 3a.[113] Compared with enzymatic electrochemical sensors, non-enzymatic electrochemical sensors have a simpler reaction mechanism. The negatively charged ZIFs composites acted as electrocatalysts and selective reagents simultaneously. The positively charged DA, UA, L-Trp or AA were attracted and electro-catalyzed on the sensor, enhancing the electron transfer rates and manifesting excellent electrocatalytic activity toward the redox reaction. The possible electrochemical reaction mechanism for oxidation is shown in Fig. 3b.

Different ZIFs materials exhibit different electrochemical mechanisms in non-enzymatic electrochemical glucose sensors to catalyze glucose to gluconolactone.[99,101–103] For example, two previous studies have reported that during anodic scanning, the cobalt based ZIFs material formed Co (OH)x for the oxidation reaction. The Co(II) species were successively oxidized to Co(III) and Co(IV) species. Subsequently, the Co(IV) species oxidized the glucose while the Co(IV) species were reduced to Co(III). The redox peaks I/II and III/IV correspond to the reversible conversion between $[Co(II)(mim)_2]_n$ and $[Co(III)(mim)_2(OH)]_n$, and $[Co(III)(mim)_2(OH)]_n$ and $[Co(IV)-(mim)_2(OH)_2]_n$, respectively.[110] The electrode process is shown in eqn (5) and (6).[101,111]

$$[Co(II)(mim)_2]_n + nOH^- \rightarrow [Co(III)(mim)_2(OH)_n] + ne^- \tag{5}$$

$$[Co(III)(mim)_2(OH)]_n + nOH^- \rightarrow [Co(IV)(mim)_2(OH)_2]_n + ne^- \tag{6}$$

There is a minor paper on non-enzymatic electrochemical adrenaline sensors. The electrocatalytic reaction mechanism is similar to that of DA, UA, and AA, and the oxidation reaction is shown in Fig. 3c.[135]

3.5 Selective detection and simultaneous detection of small biomolecules

Selectivity is another critical factor in evaluating the performance of sensors for target analytes, either enzymatic or non-enzymatic electrochemical sensing systems, especially in actual samples. Tables 1–3 show that most researchers studied the selectivity of these as-prepared electrochemical sensor platforms, they conducted the interference experiments by recording the electrochemical response.[81] There are possibilities of interfering issues by various interferences in the detection of different small biomolecules, the examples of interferences are inorganic positive ion (Na^+, K^+, Mg^{2+}, Cu^{2+}), inorganic anion (Cl^-, NO_3^-, SO_4^{2-}), amino acid (L-cysteine, leucine, glutamic acid), saccharides (sucrose, fructose, lactose, glucose), acids (citric acid, salicylic acid), some organic and biological molecules (DA, UA, AA, starch, urea, ethanol), and biogenic amines (tyramine, tryptamine, phenethylamine). It is well-known that DA, AA, and UA are small biomolecules that coexist in the biological matrix simultaneously. Therefore, any two of the compounds in DA, UA, or AA will be the interference compounds for the detection of the specific compound. Meanwhile, DA, AA, and UA will also be the main interference compounds in the detection of glucose. Therefore, it is needed to eliminate interference for an accurate detection process. The first step in developing a selective electrochemical sensor for DA is to identify suitable ZIFs materials that exhibit selective reactivity
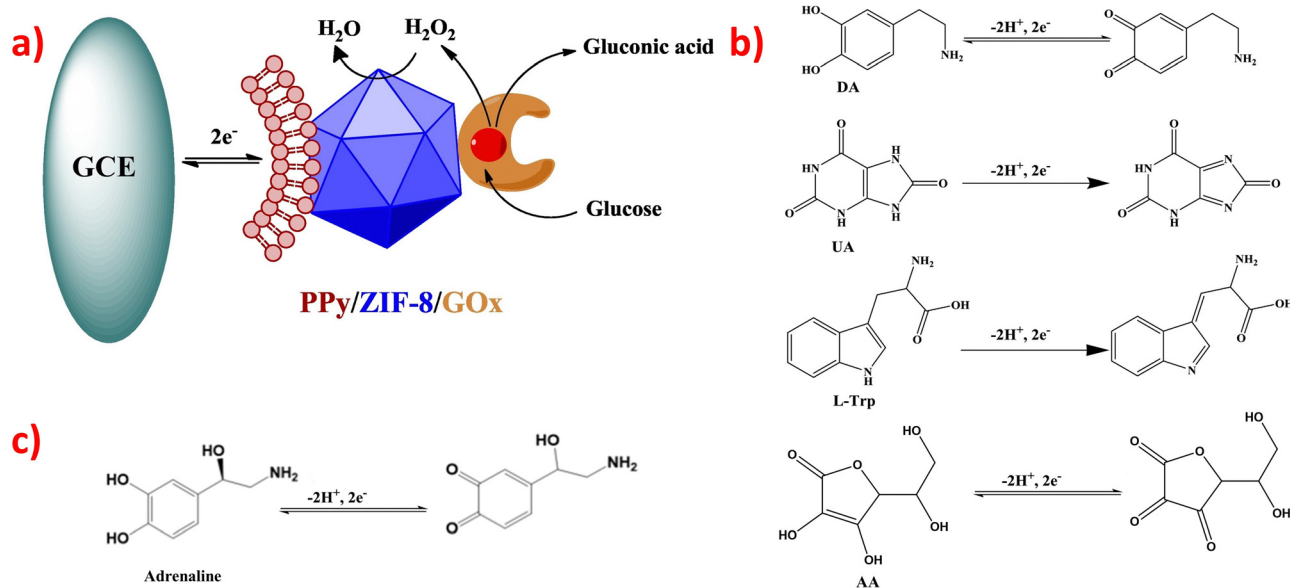

Fig. 3 (a) The mechanism of glucose detection used GOx enzyme. Reproduced with permission from ref. 113. Copyright (2018) Elsevier. (b) Reaction mechanism for DA, UA, L-Trp and AA. Reproduced with permission from ref. 81. Copyright (2019) Elsevier. (c) The reaction mechanism for adrenaline. Reproduced with permission from ref. 135. Copyright (2019) ACS.

9108 | *J. Mater. Chem. B*, 2023, **11**, 9099–9127

This journal is © The Royal Society of Chemistry 2023

towards DA. Anti-interference studies are also necessary, and can be conducted using amperometry, to confirm the performance of specific ZIFs for the selective detection of DA.[76] ZIF-67 is a 3D porous MOF based on Co^{2+} clusters and 2-methylimidazole that can easily be modified with different metal nanoparticles (such as Ag and Au) or specific functional groups (like carbon materials and conductive polymers) to form hybrid composites. The resulting ZIFs composites possess increased surface area and enhanced electron transfer rates.[78,81] The pH value is an important factor that affects the surface charge of electrodes modified by ZIFs materials. DA exists as a cationic form, while AA and UA exist as anionic forms in PBS (pH 7), and the pK_a values of DA, UA, and AA are 8.87, 5.40, and 4.10, respectively. The pK_a is a measure of the acidity of a molecule and represents the pH at which half of the molecules are protonated and half are deprotonated. The lower the pK_a, the stronger the acid and the more readily it donates a proton. This shows that the lower the pK_a, the lower its ability to donate an electron in an aqueous solution. Therefore, DA can contribute much more electrons than UA and AA due to its higher pK_a. Besides, it is easier for DA to be absorbed on the surface of the modified electrode due to the π–π stacking interaction between phenyl structures of DA and the three-dimensional imidazolate structure of ZIFs.[82] Secondly, the produced DA, UA, and AA during the physiological processes might interfere with signals during glucose detection.[98]

In principle, ZIFs contain a species with high electrical conductivity that can provide high specific surface area and abundant catalytic sites for electrocatalysis to selectively attract glucose and exclude different interfering substances. For instance, a novel electrochemical glucose sensor was fabricated by using ZIF-67-derived Co_3O_4 shells on the surface of cobalt copper carbonate hydroxide nanowires on copper foam, which demonstrated excellent electrochemical performance due to the catalytic properties of the Co_3O_4 matrix, the core–shell hierarchical nanostructures, and the high electrical conductivity of the copper foam.[99] Another example of enhancing conductivity and active sites of target composites is by using nickel foam (NF) as support, where leaf-like ZIFs are grown *in situ* and covered on the surface of NF to form stable ZIF/NF composites. These composites exhibit excellent electrochemical sensing performance and high electrocatalytic activity.[101] Besides, a molecularly imprinted electrochemical sensor for AA detection was designed by coating the surface of modified electrodes with molecularly imprinted polymers (MIPs). This sensor exhibited good stability, low preparation cost, high selectivity, and a wide application range. The use of MIPs is extremely helpful in improving the selectivity and stability for the determination of AA.[132] A dual-signal strategy was established in the developed sensor, which includes an increase in current response of tyrosine and a decrease in poly thionine. This strategy utilizes π–π stacking interactions and hydrogen bonding to recognize tyrosine and efficiently reduce potential interferences from intrinsic background electrochemical signals, resulting in improved sensitivity and accuracy. The sensor consists of Au nanoparticles metal–organic framework/poly thionine loaded with MIPs and is specifically designed for the recognition of tyrosine.[13]

After analyzing Tables 1–3, it is evident that some ZIF-based sensors have been developed for the simultaneous detection of multiple small biomolecules. Notably, a limited number of studies have reported ZIF-based sensors capable of detecting DA, UA, and AA simultaneously. The likely reason for the limited number of ZIF-based sensors capable of simultaneous detection of DA, UA, and AA is their similar structures and overlapping oxidation potentials. Therefore, finding appropriate materials to fabricate modified electrodes that can differentiate between these molecules is challenging. To address this issue, a novel electrochemical sensor (Nafion-NGR-NPC/GCE) was investigated.[59] The Nafion-NGR-NPC/GCE sensor demonstrated remarkable electrochemical activity for the simultaneous detection of DA, UA, and AA, owing to the synergistic effects of NGR and NPC. This sensor exhibited not only good conductivity but also high selectivity and low detection limit for these molecules. In addition, several studies have focused on the simultaneous detection of DA and medications such as acetaminophen or paracetamol. One possible reason for the interest in simultaneous detection of DA and medications like acetaminophen or paracetamol is that some research suggests long-term use of acetaminophen can lower the concentration of DA and potentially protect the body from stress-induced damage. This finding has significant implications for the medical field. The electrochemical behaviors of the DA and acetaminophen detection are depicted in Fig. 4a.[78] Despite extensive research in the field, very few ZIF-based sensors have been developed for the simultaneous detection of DA, UA, and L-tryptophan. The simultaneous determination of these molecules is of great significance for both research and clinical diagnosis. The electrochemical behaviors of the simultaneous detection of DA, UA, and L-tryptophan are presented in Fig. 4b.[81] Moreover, an enzyme-free sensor was synthesized by utilizing ZIF-67-derived Co_3O_4/N-doped carbon nanotube hybrids for the simultaneous detection of H_2O_2 and glucose.[105] A highly sensitive detector based on ZIF-67-derived porous Co_3O_4 hollow nano polyhedron was designed for the simultaneous detection of glucose and UA. This detector holds great potential for biological sciences.[117] An electrochemical sensor (PDMS@cZIF/GCE) was developed for the simultaneous detection of adrenaline, serotonin, and tryptophan. This innovative radiometric sensor was successfully applied to monitor the three target molecules in biological samples.[135] Thus, developing suitable ZIF materials to detect different small biomolecules simultaneously, especially those with similar structures, remains a significant challenge for scientists.

4. ZIF-carbon composites for electrochemical detection of small biomolecules

Carbon-based materials, including carbon nanotubes, carbon dots, porous carbons, graphene, and graphene oxide, have been
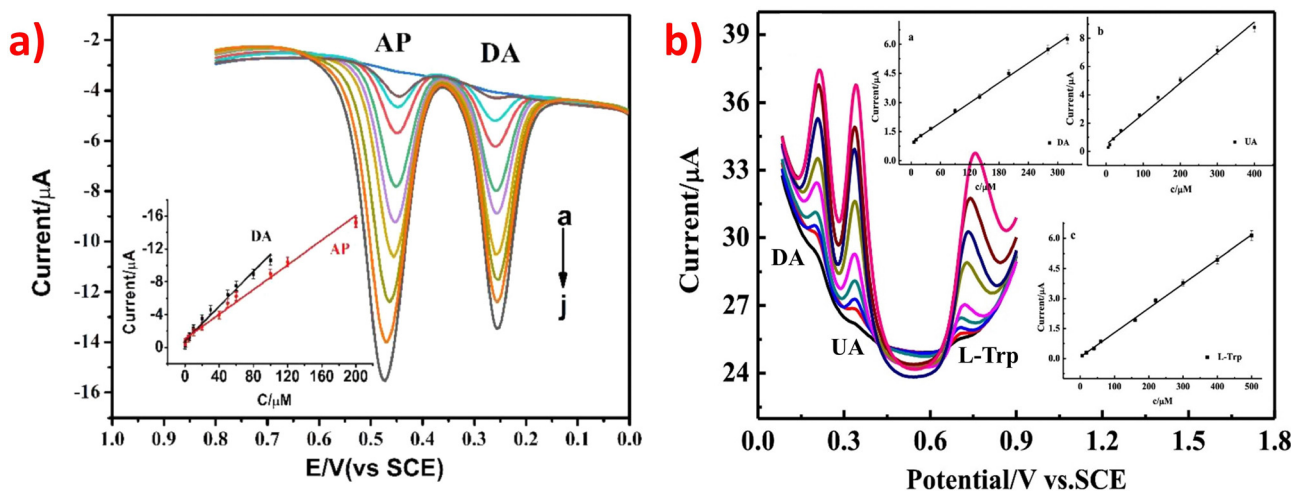
This journal is © The Royal Society of Chemistry 2023

J. Mater. Chem. B, 2023, **11**, 9099–9127 | **9109**

Fig. 4 (a) DPV profiles on Ag-ZIF-67p/GCE for the mixture of DA (0.1–100 μM) and AP (0.5–200 μM). Inset: The plots of the anodic peak currents *vs.* the concentrations of the analytes. Reproduced with permission from ref. 78. Copyright (2020) Elsevier. (b) DPV profiles on Ni-ZIF-8/N S-CNTs/CS/GCE for simultaneous detetction of DA (6.0–320 μM), UA (6.0–400 μM) and L-Trp (6.0–500 μM). Insets: The plots of the anodic peak currents *vs.* the concentrations of the analytes. Reproduced with permission from ref. 81. Copyright (2019) Elsevier.
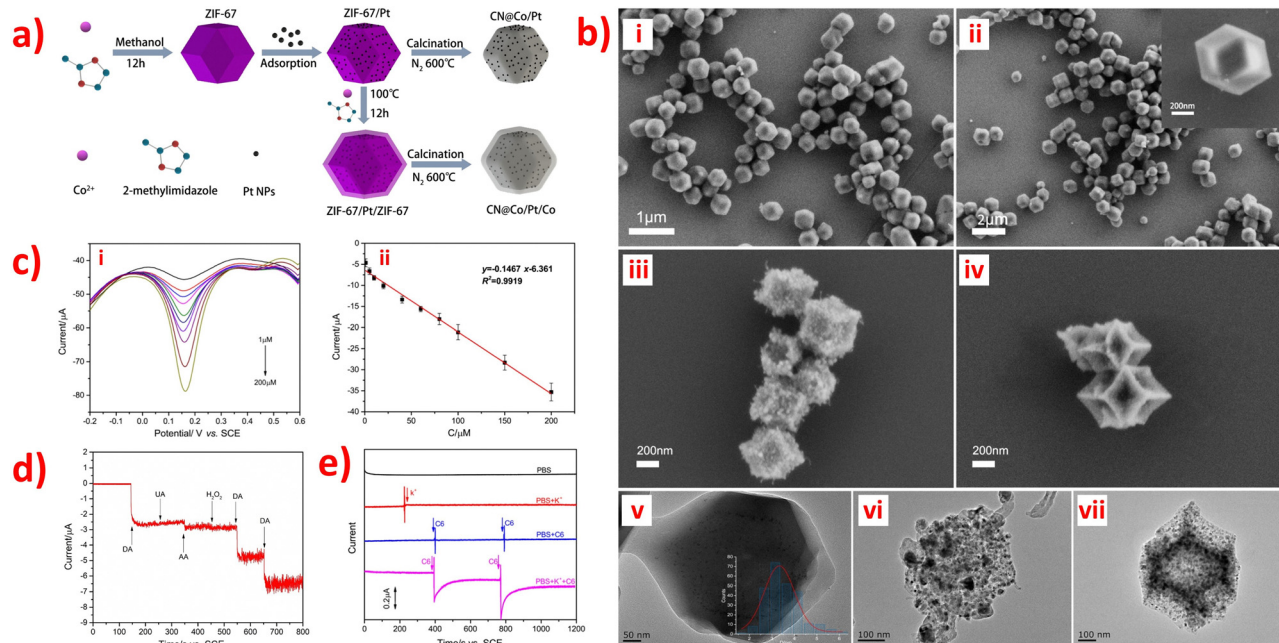
the focus of materials research and have garnered widespread interest in various fields over the past several decades.[17,19] In addition, carbon-based materials offer several advantages, including low cost, rapid electron transfer, biocompatibility, good thermal conductivity, high surface area, and high electrical conductivity.[17,159] While carbon-based materials offer many advantages, they also have some deficiencies such as poor conductivity, weak dispersibility and low solubility, which make them unsuitable for modifying electrode surfaces alone.[160,161] In contrast, ZIFs exhibit stronger hydrothermal and physicochemical properties compared to most MOFs, making them a promising choice for such applications.[77] Despite their promising properties, some pure ZIFs exhibit poor electrical conductivity, which limits their practical applications in electrochemical sensing.[86] To address this issue, a promising strategy is to combine high-conductivity carbon-based materials with ZIFs to produce ZIFs@carbon-based composites for modifying the working electrode surface. Recent studies have demonstrated that ZIFs@carbon-based composites can overcome the shortcomings of each component and enhance electrochemical performance, conductivity, and heat transfer efficiency.[162] For instance, the addition of carbon nanotubes into ZIFs can improve the mobility of charge carriers and promote the delocalization of charges, thereby enhancing electrochemical performance. Combining carbon nanotubes with ZIFs can exhibit better synergistic catalytic efficiency.[77,162] This review paper introduces various electrochemical sensors that utilize ZIFs@carbon-based composites, as follows.

4.1 ZIF-modified N-doped porous carbon materials

Nonporous carbon materials do not have porosity, which is one of the essential features of porous carbon materials. However, nonporous carbon materials do have other advantageous properties such as large specific surface area, excellent electrical conductivity, low cost, and high chemical stability that make them useful as a sensor substrate in various applications.[84,87,110] N-Doped carbon (CN) materials are promising carbon-based supporting materials due to their unique physical-chemistry properties, which exhibit outstanding sensitivity in biosensors applications and excellent electrocatalytic activity for the oxygen reduction reaction.[69,95] On one hand, CN materials offer various advantages such as diverse synthesis methods, good electron delocalization, excellent electronic transmission performance, simplicity, and diversity of preparation. These properties make them promising materials for various fields such as photocatalysis, electrocatalysis, microwave absorption, and potassium-ion storage. They also play a crucial role in stabilizing nanomaterials and catalyzing reactions.[69,110] ZIF-67 is one of the most investigated MOFs among the ZIF materials due to its large amount of active cobalt sites. Further direct carbonization of ZIF-67 can produce porous, cobalt-incorporated N-doped carbon composites.[87] The synthesis procedure of ZIF-67/Pt, ZIF-67/Pt, CN@Co/Pt and CN@Co/Pt/Co nanocomposites are shown in Fig. 5a.[84]

ZIF-modified N-doped porous carbon composites have been reported for sensing small biomolecules. An electrochemical sensor was designed by incorporating Co/Co-N nanoparticles into N-doped nonporous carbon (Co/Co-N@NPC) nanostructures and modifying carbon paste electrodes, which exhibited excellent performance for detecting DA.[87] ZIF-67 possesses a zeolitic structure with high porosity, allowing the Co²⁺ ions in ZIF-67 to be reduced to cobalt nanoparticles that catalyze the graphitization of the resultant carbons during oxidation–reduction reactions. Thus, the synergistic effects of combining Co nanoparticles with Co bonded N can result in enhanced sensitivity and selectivity for DA sensing, due to the conductive carbon and porous architecture. In this case, the Co/Co²⁺ redox couple enhances the oxidation of dopamine to dopamine-o-quinone. Moreover, the ZIF-67 derived Co/Co-N@NPC modified

9110 | *J. Mater. Chem. B*, 2023, **11**, 9099–9127

This journal is © The Royal Society of Chemistry 2023

Fig. 5 (a) Schematic illustration of the typical synthesis procedure of ZIF-67/Pt, ZIF-67/Pt,CN@Co/Pt and CN@Co/Pt/Co nanocomposites. (b) SEM images of (i) ZIF-67/Pt, (ii) ZIF-67/Pt/ZIF-67, (iii) CN@Co/Pt, (iv) CN@Co/Pt/Co, and TEM images of (v) ZIF-67/Pt/ZIF-67, (vi) CN@Co/Pt, (vii) CN@ Co/Pt/ Co. (c) (i) DPV of different concentration (1–200 μM) of DA in N_2-saturate PBS (pH 7.4) on CN@Co/Pt/Co-GCE, and (ii) Corresponding peak currents against DA concentrations (n = 3). (d) Amperometric response of CN@Co/Pt/Co-GCE (d) in PBS (pH 7.4) with the successive addition of 50 μM DA, 50 μM UA, 50 μM AA, and 50 μM H_2O_2; and (e) in PBS (black), PBS containing 50 mM KCl (red), PBS with successive addition of 100 μL of C6 cells suspension without K^+ stimulation (blue), PBS with successive addition of 100 μL of C6 cells suspension with K^+ stimulation (magenta). Applied potential: +0.185 V. Reproduced with permission from ref. 84. Copyright (2019) Elsevier.

carbon paste electrode displayed two linear ranges (10 nM to 50 μM and 50–500 μM), with a LOD of 6 nM being the best when compared to the previously reported cobalt-mediated sensors for the detection of DA. It has been independently reported that two nanocomposite materials of ZIF-67 with N-doped porous carbon or its derivatives for the detection of DA and DA, UA respectively: CN@Co/Pt/Co[84] and NCCNPs.[89] Among them, Pt nanoparticles and a hollow N-doped carbon framework were prepared to synthesize CN@Co/Pt/Co nanocomposites to modify GCE through using the electrochemical deposition method, which displayed good electron conductivity, high porosity, and large specific surface area.[84] Moreover, the uniform adsorption and dispersion of Pt nanoparticles in ZIF-67, as shown in SEM and TEM image in Fig. 5b have significantly improve conductivity and electrocatalytic activity. In addition, a DA electrochemical sensor based on CN@Co/Pt/Co showed incredibly low LOD of 2.76 nM (Fig. 5c), good anti-interference (Fig. 5d), and high-performance sensitivity and selectivity. This sensor was successfully utilized to detect extracellular DA released through C_6 cells, providing a new feasible solution for real-time monitoring of neuronal DA release, as shown in Fig. 5e.[84] Furthermore, Co and N-doped carbon particles (NCCNPs) can directly carbonize ZIF-67 to modify GCE by using the drop-casting method and electrochemically detect DA and UA, which exhibited the highest sensitivity and extremely low LOD.[89] Two aspects have been organized to explain the form and content of Co, N species can affect the detection performance,

including a large amount of Co with high crystallinity and a small amount of doped N with high electron acceptance ability, which will help design the better-modified electrodes using NCCNPs for the electrochemical detection of DA and UA. In addition, N-doped porous carbon nano polyhedral (N-PCNPs) were prepared using the direct carbonization of ZIF-8 nano polyhedral with uniform morphology, narrow pore-size distribution, high surface area, and good surface electrochemical properties.[95] And then, the nanocomposites were used to modify GCE by using the drop-casting method for the simultaneous determination of DA, UA, and AA, resulting in much larger oxidation peak separation and higher peak currents on the surface of the N-PCNPs/GCE and showing high electrocatalytic activity.

A high-performance sensor was fabricated using a nanocomposite of N-doped carbon dodecahedron embedded with Co nanoparticles (Co@NCD), which was drop-casted onto a GCE, enabling the direct electrooxidation of glucose.[98] Due to the unique morphology, large surface area, N-doped active sites, and embedded Co nanoparticles, the nanocomposite-based sensor exhibited rapid response, LOD, broad detection range, remarkable selectivity, repeatability, reproducibility, and long-term stability. Besides, three nanocomposite materials of ZIF-67 derived N-doped carbon embedded with Co_3O_4, or its derivatives, have been independently reported by distinct groups for detecting different small molecules: ZIF-67 derived Co_3O_4/NCNTs,[105] ZIF-67 derived ST-Co_3O_4,[124] and ZIF-67

derived Co_3O_4-NPCN.[136] The synthesis of ZIF-67 derived Co_3O_4/NCNTs composites and ZIF-67 derived Co_3O_4-NPCN composites involved similar steps. Both composites were obtained by carbonizing ZIF-67 under an H_2/Ar atmosphere and subsequently embedding Co_3O_4 into ZIF-67-derived N-doped carbon nanocomposites. The former composite was cooled down to 150 °C for 12 h in an oven, whereas the latter was cooled naturally down to 300 °C for 1 h under oxidative atmosphere. The ZIF-67-derived ST-Co_3O_4 materials were synthesized by a stepwise method that was proposed to construct the amorphous N-doped carbon matrix functionalized with Co_3O_4 NPs based on SiO_2 template. In addition, the amorphous carbon formed by high-temperature calcination can provide more active sites and improve the electron transport ability and dispersibility of Co_3O_4 and prevent a large amount of Co_3O_4 from agglomerating, so the as-prepared composites demonstrated good anti-interference, notable selectivity, high repeatability, robust stability, long-term stability, excellent electrochemical performance. Besides, the three sensors were fabricated by the same procedures *via* the drop-casting method, and they were all non-enzymatic sensors.
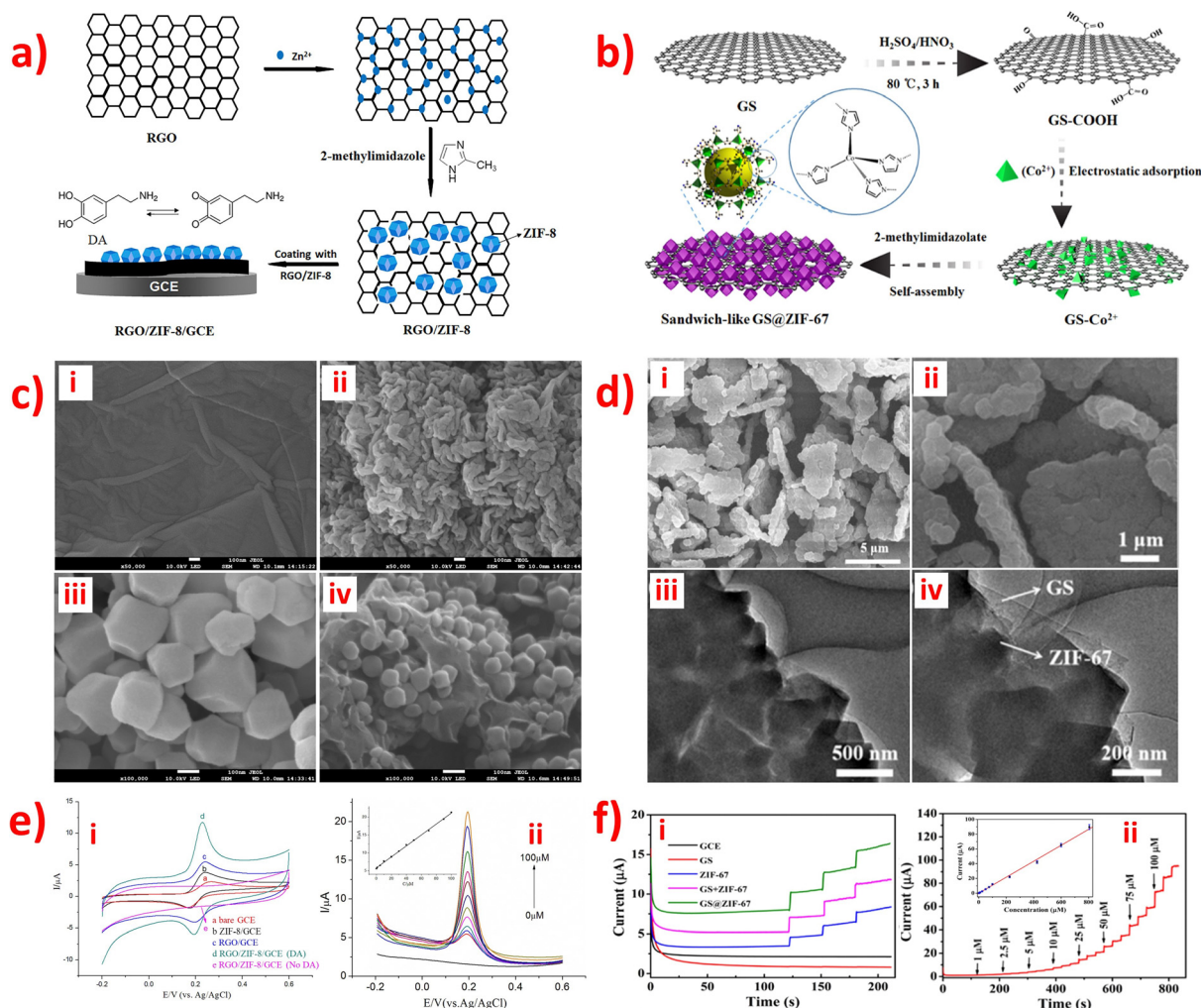
4.2 ZIF-graphene or graphene oxide materials

Graphene, a one-atom-thick planar sheet of sp^2-bonded carbon atoms arranged in a honeycomb crystal lattice, is a highly durable material for modifying electrodes in the preparation of electrochemical sensors or biosensors. Its remarkable properties make it an excellent candidate for a wide range of applications in the field of electrochemistry.[59,93] Additionally, graphene is a crucial carbon-based material with outstanding electronic conductivity, high specific surface area, exceptional electron transfer properties, high mechanical strength, and excellent chemical stability.[93,94] Usually, graphene oxide (GO) is prepared by treating graphite with strong oxidants and acids to remove excess metals, with Hummers' method being the most commonly used synthetic route. GO is considered a reliable candidate for modifying materials used in electrochemical analysis.[86] Reduced graphene oxide (rGO), a typical two-dimensional (2D) honeycomb-like carbon-based support material, is obtained by rGO, and it can easily be combined with other materials to enhance electrochemical performance. Compared to GO, rGO exhibits superior electrical conductivity and remarkable thermal stability due to the removal of oxygen-containing functional groups during the reduction process. As a result, rGO is a promising candidate for electrode materials in electrochemical sensing, with the potential to offer substantial specific surface area and be suitable for a wide range of applications.[69,79] Hence, graphene-based materials hold significant promise as novel electronic devices, such as electrochemical sensors or biosensors. The review article summarized several reports on the use of ZIF-graphene or graphene oxide materials for detecting small biomolecules in human body fluids.

Numerous research groups have developed environmentally friendly and straightforward methods to synthesize nanocomposite materials comprising ZIFs with graphene (G) or graphene oxide (GO) for modifying electrodes in the detection of various small biomolecules: GO/ZIF-67,[86] ZIF-67/rGO,[79] rGO/ZIF-8,[90] G/ZIF-8,[93] and GS@ZIF-67.[111] In contrast, GO/ZIF-67[86] and rGO/ZIF-8[90] were synthesized using an approach similar to that described for the synthesis of ZIF-67/rGO,[79] which involves the 2D rGO *in situ* growth of ZIFs (Fig. 6a). Similarly, G/ZIF-8[93] and GS@ZIF-67[111] were also synthesized using a similar method, which involves the 3D graphene *in situ* growth of ZIFs (Fig. 6b). Furthermore, these composites were fabricated on a GCE using the drop-casting method, while only GO/ZIF-67[86] was electrodeposited onto the GCE surface. The GO/ZIF-67/GCE[86] was used to simultaneously detect DA and AA using voltammetry; the ZIF-67/rGO/GCE[79] was used for the simultaneous determination of DA and H_2O_2; rGO/ZIF-8[90] and G/ZIF-8[93] were used to detect DA; GS@ZIF-67[111] was used to detect glucose. rGO/ZIF-8 nanocomposites exhibit tight particle size distribution and homogeneous particle size, which reveal the anchoring and growth of ZIF-8 nanocrystals on the RGO surfaces, as illustrated in Fig. 6c.[90] Meanwhile, the SEM images of GS@ZIF-67 manifested that 300 nm diameter of ZIF-67 crystals were uniformly coated on both sides of the GS.[111] TEM images also confirmed that graphene played the role of the substrate material and was stuck in the middle of ZIF-67 crystals with intimate contact (Fig. 6d).[111] These factors contribute to increased electron transfer and facilitate mass transfer, making them ideal for electrochemical sensing applications. The electrochemical behavior of small biomolecules at different modified electrodes was studied using the CV and CA method (Fig. 6e(i) and f(i)). The results showed that the activity of the new composites is higher than that of ZIFs, graphene, or rGO materials alone. Besides, ZIF-8 and ZIF-67 have a similar structure. Co and Zn are divalent metals, which may display similar electrocatalytic activities and electron transfer. In connection with different small biomolecules, the GO/ZIF-67/GCE,[86] ZIF-67/rGO/GCE,[79] and rGO/ZIF-8/GCE[90] have similar LODs (0.03–0.05 μm), and the G/ZIF-8/GCE[93] and GS@ZIF-67/GCE[111] have similar LODs (0.34–0.36 μm), with linear regression of $R^2 = 0.998$ (Fig. 6e(ii–iii) and f(ii–iii)). The above sensors are all non-enzymatic electrochemical devices.

In addition, some sensors have been developed using ZIFs as precursors loaded onto N-doped carbon, graphene, or rGO, or their derivatives to modify GCE or indium tin oxide (ITO) electrodes for the detection of small biomolecules. A glucose sensor was designed using the reduced graphene oxide@Co_3O_4-N-doped carbon (rGO@Co_3O_4-NC) composite, which was synthesized by an *in situ* preparation method on an ITO electrode. This was achieved by utilizing ZIF-67 as a precursor and coating rGO, followed by the template-directed growth of ZIF-67 in a confined preparation process. The non-enzymatic glucose sensor based on rGO@Co_3O_4-NC/ITO exhibited good performance due to the structural and compositional advantages of the ternary materials. The first reason is that the NC layer embedded sufficient Co_3O_4 nanoparticles as active centers and provided an excellent supporting platform for glucose oxidation. The second reason is that the conductive rGO layer, as a supporting material, increased the reduction of internal

9112 | *J. Mater. Chem. B*, 2023, **11**, 9099–9127

This journal is © The Royal Society of Chemistry 2023

Fig. 6 Schematic diagram of the preparation procedure of the (a) RGO/ZIF-8/GCE and (b) GS@ZIF-67. (c) SEM images of (i) GO, (ii) RGO, (iii) ZIF-8 and (iv) RGO/ZIF-8. (d) SEM images of GS@ZIF-67 at (i) low and (ii) high-magnification, and TEM images of GS@ZIF-67 at (iii) low and (iv) high-magnification. (e) (i) CV curves of different modified electrode of RGO/ZIF-8/GCE in 0.1 M PBS solution (pH 7.0) containing 1.0×10^{-4} M DA. (ii) DPV curves for different concentrations of DA on the RGO/ZIF-8/GCE in 0.1 M PBS solution with pH 7.0. Inset: The linear calibration plots. (f) I−t curves of (i) different modified electrode of GS@ZIF-67 in 0.1 M NaOH containing 25 μM glucose, and (ii) different concentrations of glucose at GS@ZIF-67 in 0.1 M NaOH. Inset: The linear calibration plots. Reproduced with permission from ref. 90 and 111. Copyright (2017) Elsevier. Copyright (2019) ACS.

resistance, resulting in fast charge transfer during the electro-chemical reaction. Consequently, the rGO@Co₃O₄-NC/ITO composite provided abundant active sites and wide contact areas for the adsorption and diffusion of glucose molecules, resulting in a highly efficient electrochemical reaction.[69]

Additionally, the ZIF-67 was decomposed to form Co_3O_4 and NC and understanding the structure–function relationship between rGO and NC is beneficial for the design of future nanocomposites.[59] Two types of nanocomposites, one derived from ZIF-8 and consisting of N-doped porous carbon and N-doped graphene materials, and the other derived from ZIF-67 and consisting of CoO-Co-N-doped carbon and rGO materials, were synthesized and used by two distinct groups to modify GCEs for the detection of different small biomolecules.[59] The Nafion–NGR–NPC/GCE and the CoO-Co-NC/GCE were both prepared using drop-casting methods with two-dimensional nanosheets.[59] Furthermore, the NPC was prepared by

annealing ZIF-8 under a stream of N₂ at 900 °C for 3 hours in a tube furnace, while ZIF-67-GO was pyrolyzed at 750 °C under N₂ for 2 hours. Both methods utilized exceedingly high tem-peratures to obtain the desired N-doped carbon structure. In the composites, the NPC was dispersed over N-doped graphene (NGR),[59] resulting in an adjustable physicochemical property and induced regional changes. This is due to the nitrogen element having a similar nuclear size to carbon, which can include five bonding electrons to form stable covalent bonds with the carbon element. The pyrolytic product of ZIF-8 has several advantages, including ease of manufacture, high sur-face area, good electrochemical activity, and a consistently distributed N-content in the carbon layer. The most prominent oxidation peak current (I_{pa}) was observed on the Nafion-NGR-NPC/GCE.[59] This suggests that an NPC-NGR nanocomposite, due to the coexistence of NGR and NPC with a micro and mesoporous structure, high surface area, and excellent

This journal is © The Royal Society of Chemistry 2023

J. Mater. Chem. B, 2023, 11, 9099–9127 | 9113

electrical conductivity, is beneficial for promoting electrochemical signals.[59]

However, the electronic transmission performance of CoOx is poor. Adding rGO and NC (as shown in morphology image of Fig. 7a) as support materials can improve the electrocatalytic property of CoOx nanostructures to obtain high-performance materials for electrochemical detection of glucose. This is because rGO and NC have excellent electronic transmission performance and excellent physical chemistry properties. In Fig. 7b, the CVs of bare GCE, CoO-Co-NC/GCE, and CoO-Co-NC-rGO/GCE electrodes in the presence and absence of glucose are shown. Notably, the current response intensity of the CoO-Co-NC/GCE electrode for 2 mM glucose is lower than that of CoO-Co-NC-rGO/GCE. This phenomenon indicates that the CoO-Co-NC-rGO has better sensing performance than CoO-Co-NC for electrochemical detection of glucose due to the presence of rGO, which improves the electro-catalytic activity of CoO-Co-NC and facilitates the electron transfer kinetics. The unique material structure of CoO-Co-NC-rGO nanosheets enables high-performance non-enzymatic electrochemical detection of glucose.[110] Also, the presence of CoOx nanostructures in the CoO-Co-NC-rGO/GCE has an impact on the electronic transmission performance of the entire sensor. Additionally, a novel amperometry glucose biosensor was designed based on the GOx/PDA/ZIF-8@rGO composites, and its synthesis route was overly complicated.[122] The synthesis process for the GOx/PDA/ZIF-8@rGO composites involved the construction of $CaCO_3$@PDA/ZIF-8 microcapsules using $CaCO_3$ templates, followed by the addition of reduced graphite oxide nano-sheets (rGO) to remove $CaCO_3$ microparticles and obtain PDA/ZIF-8@rGO microcapsules. The GOx/PDA/ZIF-8@rGO composites were obtained by immobilizing GOx into PDA/ZIF-8@rGO microcapsules, thereby creating a mimetic multi-enzyme system. The GOx/PDA/ZIF-8@rGO/GCE was prepared using the drop-coating method, with the following mechanism: glucose was first infiltrated into the PDA microcapsules, and then catalyzed by GOx to produce glucose acid and H_2O_2. Next, ZIF-8 catalyzed the H_2O_2 to H_2O by receiving and losing electrons when in contact with the electrode. The addition of rGO enhanced the electrochemical activity, accessible surface area, and conductivity of ZIF-8 by promoting electron exchange from ZIF-8 to the electrode through cooperative interactions, such as π–π stacking and hydrogen bonding, between rGO and ZIF-8. Finally, the PDA/ZIF-8@rGO/GCE exhibited higher oxidation current than the bare GCE and PDA/ZIF-8/GCE, indicating that the combination of rGO and ZIF-8 can improve sensitivity and provide excellent electrocatalytic activity towards H_2O_2. The combination of rGO and ZIF-8 is a promising strategy for the development of highly sensitive, selective, stable, and anti-interferential electrochemical biosensors for glucose detection. In addition, a novel non-enzymatic sensor for the detection of adrenaline (Ad) was developed using a nitrogen-rich carbon-coated ZIF-67 embedded three-dimensional graphene (ZIF-67/NC/3DG) fiber.[136] Firstly, polypyrrole was used as a precursor for NC, which was then connected to ZIF-67 and the 3DG fiber electrode. ZIF-67 was able to adsorb Ad through hydrogen bonding and electrostatic interactions. Moreover, the ZIF-67/NC/3DG fiber electrode was prepared using a facile one-pot electrodeposition self-assembly method. Thus, the addition of highly conductive NC improved the sensitivity of the
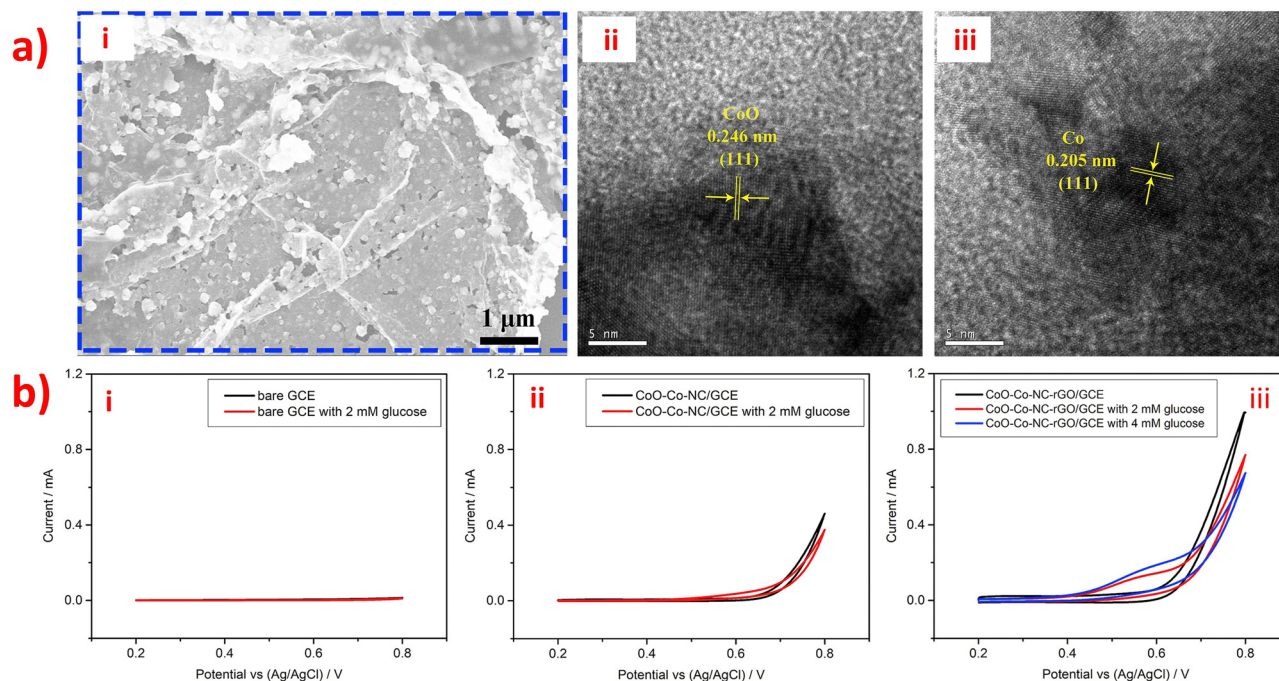

Fig. 7   (a) (i) SEM image and (ii–iii) HRTEM of the CoO-Co-NC-rGO nanocomposites. (b) CV of glucose at (i) bare GCE, (ii) CoO-Co-NC/GCE and (iii) CoO-Co-NC-rGO/GCE. Reproduced with permission from ref. 110. Copyright (2018) Elsevier.

9114 | J. Mater. Chem. B, 2023, **11**, 9099–9127

This journal is © The Royal Society of Chemistry 2023

constructed fiber sensor, while the use of 3DG enhanced the surface area, conductivity, and electrochemical stability of the complete system. Furthermore, Polypyrrole (PPy) is a type of conjugated polymer that exhibits good affinity between MOFs and graphene. The ZIF-67/NC/3DG fiber electrode showed the most extensive oxidation peak current towards Ad, which was higher than that of the bare 3DG, ZIF-67/3DG, and NC/3DG fiber electrodes. Thus, the ZIF-67/NC/3DG fiber was a promising electrode material for micro-detection systems.

4.3 ZIF-derived carbon nanotubes (CNTs) materials

Carbon-supported materials, especially carbon nanotubes (CNTs), have garnered significant interest in electrochemical sensing owing to their exceptional chemical and mechanical properties, high thermal and mechanical stability, large surface area, unique electronic structures, excellent electronic conductivity, good biocompatibility, and ultra-light weight.[77,81,163] CNTs are particularly suitable for enhancing electrical activity, serving as high-conductivity carbon materials, and providing structural support for nanocomposites in sensing applications.

When doped in ZIFs to form composite materials, they increase conductivity and provide high sensitivity for electrochemical sensing. The addition of CNTs to ZIFs resulted in composite materials that exhibited the characteristics of each component, with CNTs providing high conductivity and structural support, and ZIFs providing enhanced sensitivity for electrochemical sensing. They showed the synergistic effect because of the interfacial interactions in various parts through compact bonding and conjugation. It has been reported that carbon nanotube-doped electrode materials can increase the electrochemical peak intensity and reduce the detection limit of some small biomolecules. For example, an electrochemical sensor was designed for the detection of DA based on HP-ZIF-8/3DCNTs nanocomposites using a facile method. The method involved polymerizing zinc ions and 2-methylimidazole in the aqueous phase of a micelle formed by a sodium dodecyl sulfate (SDS) and diethylene glycol monoethyl ether (DEGEE) aqueous solution to grow HP-ZIF-8 *in situ* on the 3DCNTs template.[77] The compound consists of ZIF-8 and three-dimensional carbon nanotubes (3DCNTs) and fabricated a GCE through drop-
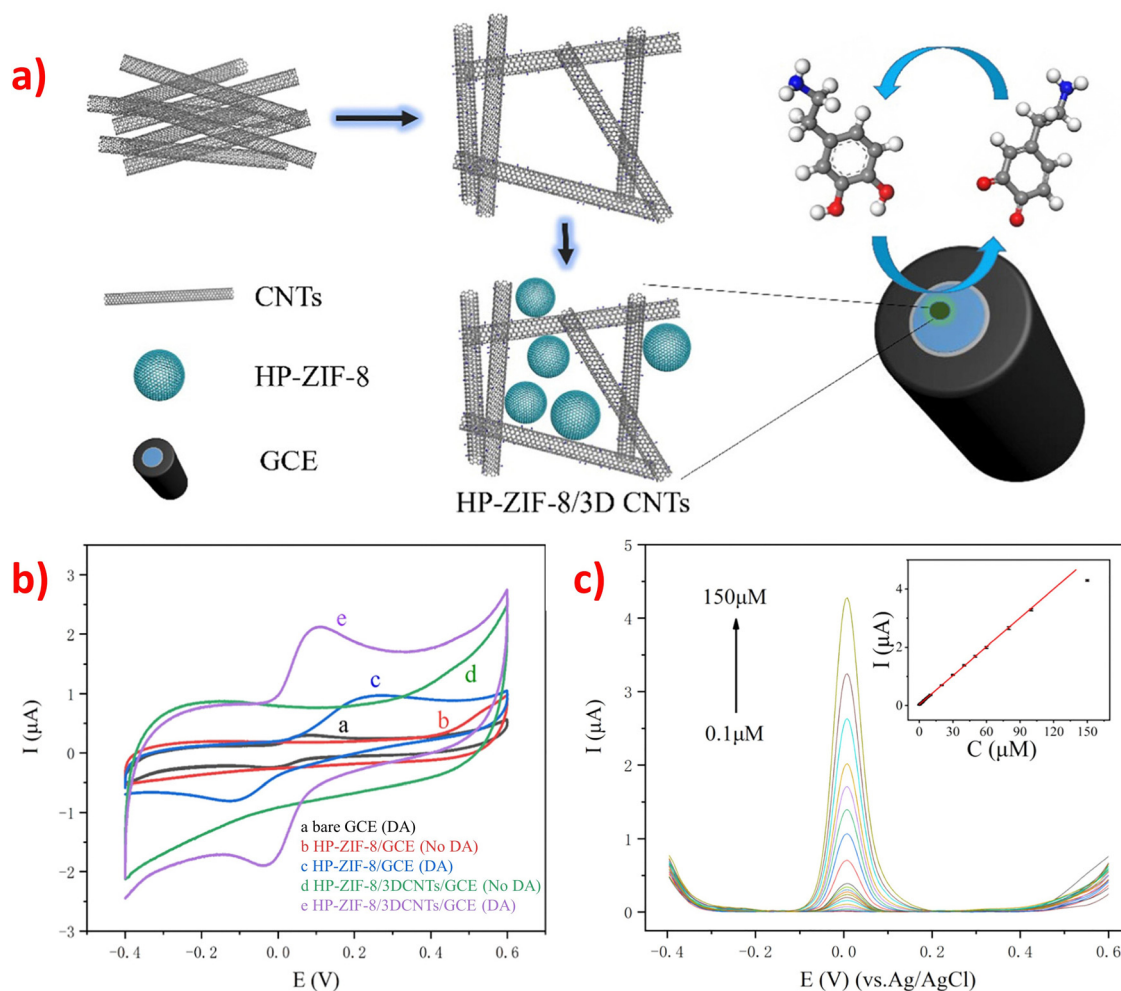
Fig. 8 (a) Preparation process diagram of the HP-ZIF-8/3DCNTs/GCE. (b) CV test patterns of HP-ZIF-8/3DCNTs/GCE modified electrode with and without 50 μM DA. (c) DPV curves of the HP-ZIF-8/3DCNTs/GCE at several concentrations of DA in 0.1 M PBS solution (pH 6.0). Inset: The linear relation between the response currents and the content of DA added. Reproduced with permission from ref. 77. Copyright (2020) Elsevier.

This journal is © The Royal Society of Chemistry 2023

J. Mater. Chem. B, 2023, **11**, 9099–9127 | **9115**

casting methods (Fig. 8a). It is clearly obvious that the curve of HP-ZIF-8/3DCNTs composite has obvious redox pairs and the peak current performance (curve d) is better than HP-ZIF-8, which is attributing to electrocatalytic performance enhancement synergistically through the recombination of 3DCNTs and ZIF-8 (Fig. 8b). With the unique structure, high conductivity, large surface area of CNTs, and extensive hierarchical porosity of HP-ZIF-8, the synthesized HP-ZIF-8/3DCNTs composite electrode exhibited better electrocatalytic activity and higher current intensity than the HP-ZIF-8 electrode for the detection of DA due to the synergistic effect of 3DCNTs and HP-ZIF-8. The response current of DA increases with the aggrandizement of DA concentration, and there is an excellent linear dependence between the current intensity and DA content, as depicted in the inset of Fig. 8c, with the LOD of 2.7×10^{-8} M (S/N = 3).

A simple electrochemical sensor was fabricated based on the ZIF-65@CNTs nanohybrid,[133] and a novel Ni-ZIF-8/NS-CNTs/CS sensing device[81] was constructed to modify electrode through a simple physical ultra-sound method. The ZIF-65@CNTs nanohybrids were synthesized using an *in situ* synthesis method, where ZIF-65 was immobilized onto the surface of carboxylate CNTs. The resulting nanocomposites were then drop-coated onto a GCE to form a modified electrode. This electrode exhibited a lower LOD and wider linear range and showed sensitive detection performance for the detection of AA compared to other similar composites. Different research groups have prepared Ni-ZIF-8/N S-CNTs/CS composites, where Ni-ZIF-8 was used to provide excellent surface area, and N S-CNTs and CS were used to improve conductivity and stability. These composites exhibited superior electrocatalytic activity, lower detection limit, and broader linear range for the simultaneous determination of DA, UA, and L-tryptophan. In addition, it can be concluded that CNTs are an excellent carbon material and can enhance the sensitivity of the electrochemical sensor. However, it has been reported that the design and preparation of ZIF-CNTs composite materials have not been widely explored for the electrochemical detection of small biomolecules. An electrochemical sensor was developed using multi-walled carbon nanotubes (MWCNTs)-based buck paper (BP) as a high-conductivity and mechanically robust material. The CoP/Co-BP/SCE electrode was fabricated by electrodepositing a uniform layer of ZIF-67 onto the surface of BP and immersing BP into ZIF-67 through a slow crystal growth process, which is a more complex approach compared to a simple drop-casting method, and provides better coverage of the electrode surface.[105] One plausible reason for the successful synthesis of uniform ZIF-67 layer on the surface of MWCNTs-based buck paper (BP) is that the carboxyl groups of MWCNTs can coordinate freely with Co^{2+} to form a center, thereby triggering the growth of ZIF-67 to obtain a uniform layer. Therefore, CoP and BP can be combined powerfully to synthesize better CoP/Co-BP composites *via* the above method, and these composites can show excellent electrocatalytic performance for glucose sensing due to the superior electrical conductivity and catalytic performance of the CoP. And then, the CoP/Co-BP materials synthesized using the above method were found to have a larger surface area and more

active sites, making them a promising candidate in the field of implantable biosensors in the future.

4.4 ZIF-derived porous carbon materials

The use of porous carbon as a sensing platform and in electroanalytical chemistry has attracted considerable interest due to its low cost, high electron conductivity, extremely high specific surface area, strong chemical stability, abundant availability, ease of surface functionalization, high sensitivity, wide detection range, and good catalytic performance.[8,129,134] Two kinds of ZIFs-derived porous carbon (PC) nanocomposites have been reported for the detection of glucose: Ni/NPC[115] and H-ZDPC.[118] Ni/NPC/GCE was successfully obtained *via* electrodeposition method, which was used to put nickel nanoparticles deposition on N-doped porous carbon modified GCE surface, and it was a non-enzymatic biosensor (Fig. 9a). It is clearly visible from the SEM images that NPC evidently thicker and smooth before the nickel deposition and after existing sheeted (Fig. 9b(i)). Fig. 9b(ii) performed that Ni/NPC hold its original shape with rough surface. However, for H-ZDPC/SPCE, it was prepared using a drop-casting method, where ZIF-67 precursors were used to synthesize ZIF-67-derived porous carbon, which was then treated with hydrochloric acid (HCl) to remove Co nanoparticles. Afterwards, glucose oxidase (GOx) was immobilized on the H-ZDPC modified SPCE through physical adsorption to create an enzyme sensor platform. Compared with bare GCE, NPC/GCE, and NiNPs/GCE, Ni/NPC/GCE exhibited superior electrocatalytic behavior towards the oxidation of glucose (Fig. 9c). Compared to ZDPC/SPCE, H-ZDPC/SPCE exhibited larger redox peaks, provided a stable platform for enzyme immobilization, and preserved the enzyme's bioactivity. However, Ni/NPC/GCE displayed higher sensitivity, lower detection limit, and wider linear range for glucose sensing than GOx/H-ZDPC/SPCE, indicating that the electrochemical performance of glucose is affected by the type of ZIF material, the type of electrode, the testing theory of non-enzymatic sensors, and the immobilization of enzymes.

There are two types of electrochemical sensors mentioned: one is a nanozyme biosensor that is based on bimetallic nanoparticles decorated with hollow nonporous carbon (Au/Co@HNCF/GCE),[127] and another one was a non-enzymatic sensor based on bimetallic ZIFs derived porous carbon (CNCo/GCE)[129] for the detection of UA. The two sensors were fabricated by the drop-casting method. At the same time, Au/Co@HNCF/GCE was constructed by pyrolysis of the Au(III)-etching ZIF-67, and CNCo/GCE was prepared *via* direct carbonization of a BMZIF nanocrystal. Although the two sensors both detected the same small biological molecule (UA), their composites with porous carbon presented different electrochemical behaviors and LODs (0.023 *vs.* 0.83 μM). Mainly because of the electrocatalytic activity of the nanozyme biosensor was better than that of the non-enzymatic sensor, another critical reason was that the bimetallic nanoparticles Au NPs and Co NPs combined with the porous carbon framework, enhancing higher activity for UA oxidation, and generating superior
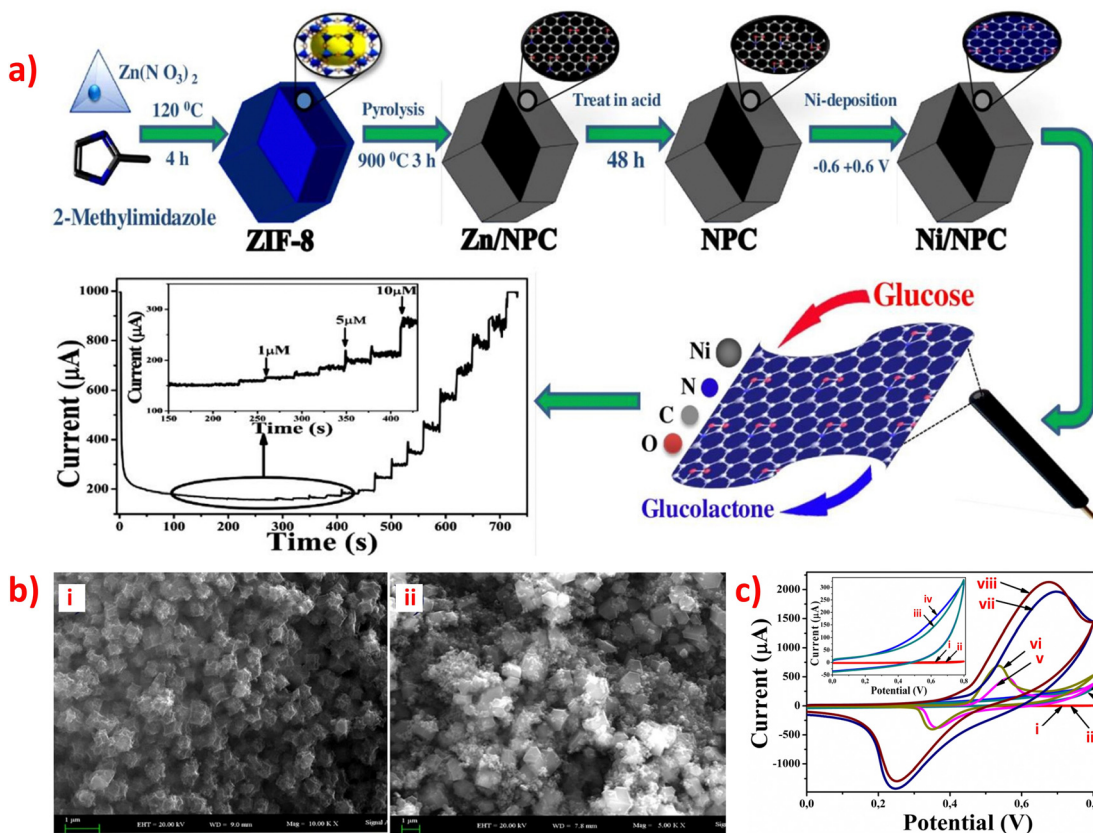
Fig. 9 (a) Schematically nanomaterial preparation of Ni/NPC and its application for glucose determination. (b) SEM image of the (i) NPC and (ii) Ni/NPC nanocomposites. (c) CV of different electrodes with absence of glucose: (i) GCE, (iii) NPC/GCE, (v) NiNPs/GCE, (vii) Ni/NPC/GCE and with presence of 0.1 M glucose: (ii) GCE, (iv) NPC/GCE, (vi) NiNPs/GCE, (viii) Ni/NPC/GCE in 0.1 M KOH. Inset: GCE (i) and (ii) and NPC/GCE (iii) and (iv) at scan rate of 100 mV s^{-1}. Reproduced with permission from ref. 115. Copyright (2020) Elsevier.

signals compared to the bimetallic ZIFs-derived N, Co-doped porous carbon.

At last, two complicated composites with ZIFs derived porous carbon to detect different small biological molecules: N-CF@N, P-CF,[8] and Fc (COOH)$_2$/ZIF-8/3D-KSCs,[134] which were both using common ZIF-8 as the precursor. Corrected sentence: N-CF@N, P-CF/GCE were prepared by using multi-heteroatoms doped yolk–shell porous carbon instead of N-doped porous carbon, which exhibited significantly increased surface area, improved pore size distribution, active electrochemical area, electron transfer kinetics, and provided more active sites. Furthermore, N-CF@N and P-CF/GCE were prepared using the drop-coating method with mixed multi-heteroatoms doped yolk–shell porous carbon. The former consisted of an N-doped carbon core, while the latter had an N,P-co-doped carbon shell. The electrochemical sensing platform based on N-CF@N, P-CF/GCE exhibited good sensitivity and selectivity towards various target molecules, including organic pollutants (hydroquinone and catechol), pharmaceutical molecules (acetaminophen), and small biological molecules (DA and UA), with LODs of 15.4 nM, 18.8 nM, 16.2 nM, 22.2 nM, and 24.5 nM, respectively. However, the Fc (COOH)$_2$/ZIF-8/3D-KCSs nanocomposites were composed of ferrocene dicarboxylic acid (Fc (COOH)$_2$), zeolitic imidazolate framework-8 (ZIF-8), and three-dimensional (3D)

kenaf stem-derived microporous carbon (3D-KSCs). Moreover, the electrochemical biosensor was prepared via the electrode-position method with the electrical connection of 3D-KCS and graphite powder. At the same time, Fc (COOH)$_2$/ZIF-8 grew on 3D-KSCs and can improve the CVs signals to AA, and the phenomenon of a wide detection range, low LOD, good stability, and selectivity can also be observed for the composites. The study demonstrated that using 3D-KSCs as a matrix to support ZIF-8 on the surface can provide suitable electrical conductivity, a large specific surface area, and many active catalytic sites, resulting in excellent catalytic performance for AA detection. This approach could pave the way for synthesizing ZIF-8-based nanocomposites for electrochemical sensors.

5. ZIF-metal-based composite for electrochemical detection of small biomolecules

Nano-sized precious metal nanoparticles (NPs), such as Pt, Au, Ag NPs, metal oxides (Co$_3$O$_4$, Fe$_3$O$_4$), and ZIF-derived bimetallic composites (Cu–Co, Co–Fe) have attracted tremendous interest for the studies of some small biomolecules due to their extraordinary catalytic properties.[100] Therefore, they are suitable

This journal is © The Royal Society of Chemistry 2023

J. Mater. Chem. B, 2023, 11, 9099–9127 | 9117

candidates for combining with ZIFs to form nanocomposite materials and using them to create electrochemical sensors for detecting various small biomolecules in human body fluids. It has been summarized that ZIFs-derived metal nanoparticles, bimetallic composites, and metal oxide composites can be used to develop electrochemical sensing devices that can be applied to various fields.
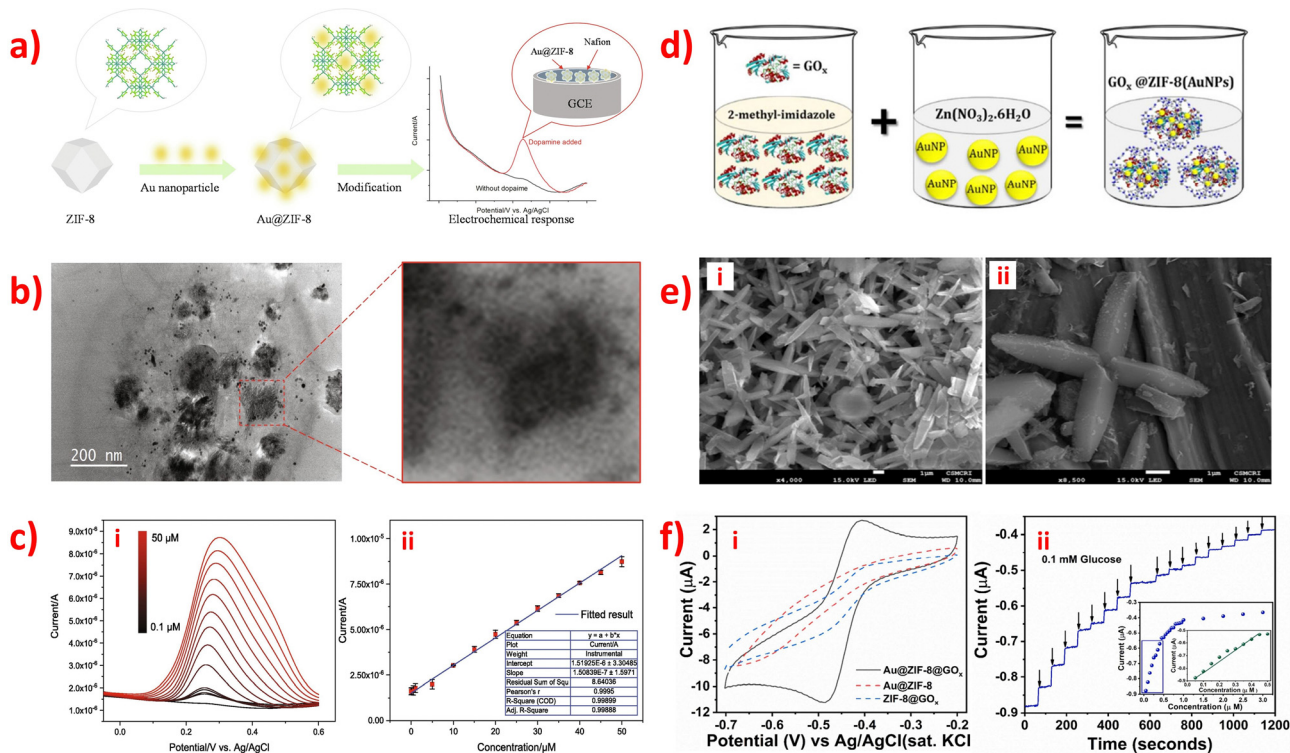
5.1 ZIF-derived metal nanoparticles

Many papers have reported the use of ZIFs in electrochemical biosensing, but porous ZIFs (such as ZIF-8 with specific pore sizes to accommodate biomolecules and protect them from external stimuli) have drawbacks such as poor conductivity and weak electrocatalytic ability, which hinder their electrochemical applications. In addition, directly fabricating the prepared porous ZIFs onto electrode surfaces often results in uneven modification or excessive film thickness, which can limit their effectiveness.[114,131] To address these issues, researchers have suggested incorporating highly electrically conductive and electroactive materials into ZIFs to improve the sensitivity of the sensors. Metal nanoparticles, with their high conductivity and excellent electrocatalytic activity, are easily combined with ZIFs to form nanocomposites.[80,131] In addition, the introduction of metal nanoparticles can increase the surface area, which leads to a reduction in the tunneling distance for electrons and an increase in the surface conductance of the electrode, facilitating efficient charge transfer to the electrode surface.[114] The combination of ZIFs and metal nanoparticles can enhance electrochemical activity due to the unique properties of each component and their synergistic effect, leading to the development of electrochemical biosensors with excellent detection performance for various small biomolecules.[162] In terms of these above features, many hybrids were used to fabricate electrochemical sensors and various fields, including electroanalytical chemistry.[80] Among the more commonly used metal nanoparticles, gold (Au), silver (Ag), copper (Cu), and platinum (Pt) NPs are the four most widely studied.

First, gold (Au) nanoparticles possess several unique features, including small size, large surface area, biocompatibility, molecular recognition, high surface activity, and good conductivity. These critical characteristics of Au nanoparticles can significantly influence electrocatalytic activity.[142,162] For example, a non-enzymatic DA sensor was prepared based on Au@ZIF-8 nanocomposites, which were synthesized by using a solution of Au NPs mixed with ZIF-8 nanocomposites through a simple solvothermal method.[80] It is worth noting that the Au NPs are well-distributed on the inner surfaces of the ZIF-8 nanocrystals, as confirmed by Fig. 10a. The Au@ZIF-8 nanocomposites exhibit a monodisperse, polyhedral shape, and the ZIF-8 nanocrystals provide a larger surface area for Au NPs, as shown in Fig. 10b. The electrochemical detection performance of Au@ZIF-8/GCE toward DA depicted a comparable sensitivity (6.452 μA mM^{-1} cm^{-2}) and lower LOD (0.01 μM (S/N = 3)) (Fig. 10c). This may be due to the high conductivity which is essential to the enhancement of electrocatalytic to the detection of DA. Another example is the mediator-free enzymatic glucose

sensor of GOx@ZIF-8(AuNPs)/GCE.[114] The GOx@ZIF-8(AuNPs) nanocomposites were synthesized through a process of encapsulating gold nanoparticles and glucose oxidase into the cavity of ZIF-8 (Fig. 10d). The catalyst can then oxidize glucose to gluconate through the catalysis of glucose oxidase (GOx), leading to the production of H_2O_2. The redox stability of the FAD/FADH2 redox couple is a significant advantage in the fabrication of the catalyst. The morphology of the GOx@ZIF-8(AuNPs) nanocomposites was observed to have a star-shaped morphology of ZIF-8 microstructure at low magnification and an assembly of rod-like star morphology at high magnification (Fig. 10e(i–ii)). These unique morphologies of the composite are suggested to be caused by the affinity of GOx towards imidazole-containing structural units (ZIF-8) due to intermolecular H-bonding.[114] Compared to ZIF-8@GOx, both Au@ZIF-8 and GOx@ZIF-8(AuNPs) showed better electrocatalytic behavior towards the oxidation of glucose (as shown in Fig. 10f(i)), indicating a significantly high electron transfer rate of the reversible redox equilibrium of the FAD/FADH$_2$ redox couple. Therefore, the sensor's sensitivity could be up to 10-fold and having a detection limit of 50 nM of glucose (Fig. 10f(ii)) because of the incorporation of Au NPs, shortening the electron tunneling distance by mediating the charge. At last, these two sensors were fabricated by the drop-casting method. They presented a broader detection range, lower LOD (limit of detection), high sensitivity, excellent selectivity, long-term stability, and good reproducibility for the determination of DA and glucose, respectively.

Another important metal nanoparticle is AgNP. Ag nanoparticles possess excellent characteristics of high conductivity and biocompatibility, which have attracted a lot of attention in the field of Ag-containing electrochemical sensors, similar to Au nanoparticles.[78,116] It has been reported that three types of sensors based on ZIF-67 with Ag nanoparticles, or their derivatives have been developed for the detection of small biomolecules, such as DA and glucose: Ag@ZIF-67/GCE,[116] Ag-ZIF-67p/GCE,[78] and Ag@ZIF-67/MWCNT.[123] Among them, the simplest sensors were Ag@ZIF-67/GCE and Ag-ZIF-67p/GCE, which had similar electrode material composition. At first, AgNPs were encapsulated into the Co-based porous MOF $[Co(mim)_2]_n$ (denoted as ZIF-67, mim = 2-methylimidazole) by a sequential deposition-reduction method to form Ag@ZIF-67/GCE for the detection of glucose and the detailed reaction process as follows: the desolated ZIF-67 and Ag$^+$ were both dispersed in the ethanol solution using Ag$^+$ as the precursors, and then produced the reduction reaction by $NaBH_4$ to yield Ag@ZIF-67 nanocomposite (Fig. 11a).[116] The electrooxidation process was main firstly performed by oxidizing $[Co(II)(mim)_2]_n$ to $[Co(III)(mim)_2(OH)]_n$ and further to $[Co(IV)(mim)_2(OH)_2]_n$, and then glucose carried out oxidation reaction at the cost of $[Co(IV)(mim)_2(OH)_2]_n$ consumption, leading to the current change. However, the synthesis process of Ag-ZIF-67p[78] was the same as that of Ag@ZIF-67[116] except adding ultrasonication for 1 h to obtain ZIF-67 nano Pinnas (ZIF-67p) (Fig. 11d), which was used for the detection of dopamine (DA) and acetaminophen (AP). Moreover, compared with Ag@ZIF-67 particles,

9118 | J. Mater. Chem. B, 2023, 11, 9099–9127

This journal is © The Royal Society of Chemistry 2023

Fig. 10 (a) Illustration of synthesis of Au@ZIF-8 nanocomposite and its electrochemical response toward DA. (b) TEM image of Au@ZIF-8 nanocomposites and the enlarged area. (c) (i) DPV of DA with increasing concentration, and (ii) the relationship of the oxidation peak current (I_{pa}) with the concentration of DA. Reproduced with permission from ref. 80. Copyright (2020) Elsevier. (d) Synthesis of GOx@ZIF-8(AuNPs). (e) FESEM image of 5nm gold coated GOx@ZIF-8(AuNPs) (i) crystalline growth and (ii) single particle showing large surface area. (f) (i)CV of ZIF-8@GOx, Au@ZIF-8 and GOx@ZIF-8(AuNPs) at a scan rate of 0.1 V s^{-1} in N$_2$ saturated 0.1 M pH 7.4 PBS. (ii) I–t measurement of catalytic glucose oxidation at -0.45 V vs. Ag/AgCl (sat. KCl) with successive addition of 0.1 mM glucose. Inset: Calibration plot of concentration versus (full and linear region) current. Reproduced with permission from ref. 114. Copyright (2018) ACS.

Ag@ZIF-67p had a smaller size that could increase active surface area and unique morphology that could improve the active site and the Ag NPs loading (Fig. 11b and e). Meng et al. also studied the transient response curves of Ag@ZIF-67/GCE with 0%, 0.1%, 0.2%, 0.5%, and 0.8% Ag, and it could be seen that the Ag-0.5%@ZIF-67GCE showed the best electrocatalytic performances towards glucose oxidation because of the additions of Ag content could improve the conductivity and charge transportability of ZIF-67, as shown in Fig. 11c. In addition, it was noted that the oxidation current of DA and AP at the Ag-ZIF-67p/GCE exhibited an increased current signal, much higher than that of bare GCE, ZIF-67p/GCE, and Ag-ZIF-67/GCE (Fig. 11f). In short, these two sensors displayed high selectivity, long-time stability, good reproducibility, and low LODs. At last, a sensor was designed based on the Ag@ZIF-67/MWCNT nanocomposites by using ZIF-67 to encapsulate Ag NPs and on the surface of ZIF-67 multi-walled carbon nanotubes (MWCNTs).[123] Furthermore, Ag@ZIF-67/MWCNT constituted rich metallic centers, possessed a substantial specific area, and had multiple valence states, this sensor showed an improved catalytic activity toward glucose.

In addition, an electrochemical sensor for the detection of AA was prepared by in situ growth of a ZIF-8 membrane on the surface of a GCE modified with platinum nanoparticles (PtNPs)

using an electrodeposition method, resulting in a ZIF-8/Pt NPs/ GCE.[131] The Cu-in-ZIF-8-based electrochemical sensor was prepared by encapsulating CuNPs in ZIF-8 and further modifying them onto the surface of a screen-printed electrode (SPE) for nonenzymatic sensing of glucose using a drop-casting method. Additionally, two different sensors were developed by encapsulating metal nanoparticles in the ZIF-8 shell, namely Cu-in-ZIF-8 and ZIF-8/Pt NPs/GCE, due to the high conductivity and electrocatalytic activity of CuNPs and PtNPs. The composites were easily formed with ZIF-8 and helped overcome the poor heterogeneous nucleation ability of ZIF-8, resulting in improved sensing performance. Both sensors showed good sensitivity, selectivity, and reproducibility when detecting AA and glucose, respectively.

5.2 ZIF-modified metal oxide NPs materials

Metal oxides (such as Fe_3O_4, TiO_2, and Co_3O_4) have some advantages of non-toxicity, high surface area, and electrocatalysis, but their use remained limited due to their low conductivity.[100] To enhance the conductivity, combining ZIFs with metal oxides or other highly conductive materials is needed to form new nanocomposites to detect different small biomolecules in human body fluids. Among various metal oxides, TiO_2 nanostructures have attracted greater attention.
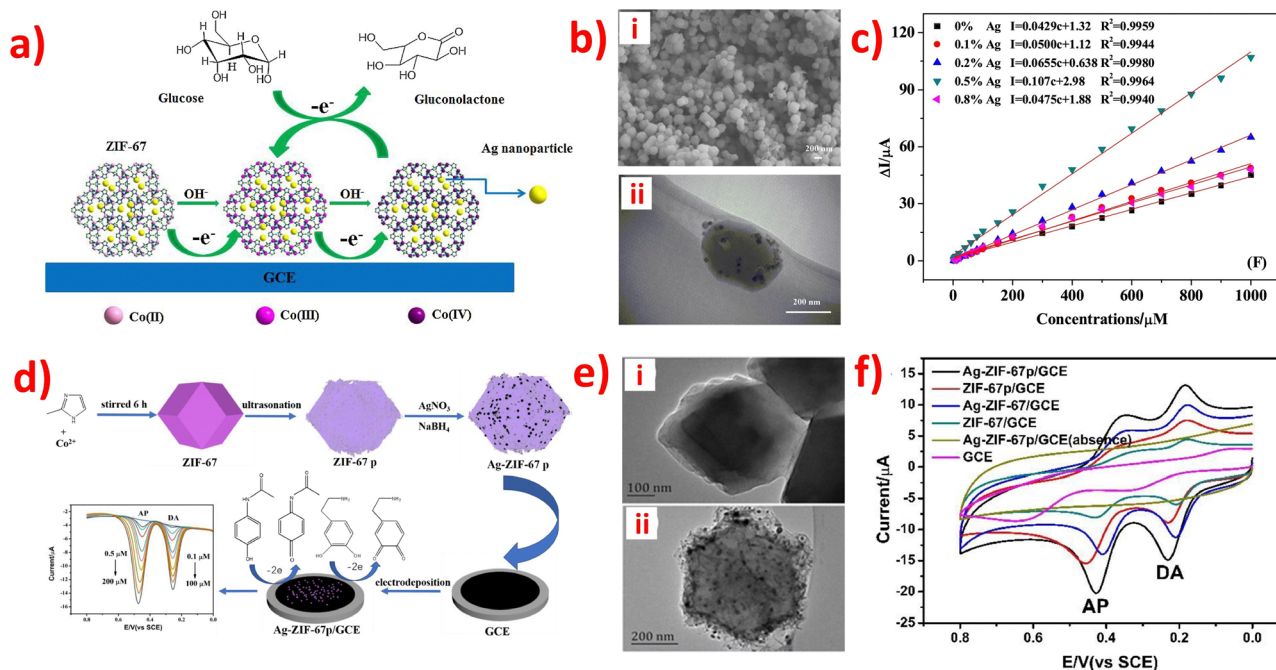
Fig. 11 (a) Schematic illustration of the electrooxidation of glucose to gluconolactone by Ag@ZIF-67 modified GCE in NaOH solution. (b) (i) SEM and (ii) TEM image of Ag@ZIF-67. (c) The relationships between glucose concentration and current signal of Ag@ZIF-67/GCE with 0%, 0.1%, 0.2%, 0.5% and 0.8% Ag. Potential: 0.42 V. Reproduced with permission from ref. 116. Copyright (2018) Elsevier. (d) The fabrication of Ag-ZIF-67p modified GCE and the application of AP and DA detection. (e) The TEM of the (i) ZIF-67p and (ii) Ag-ZIF-67p. (f) CVs at the bare GCE, ZIF-67/GCE, ZIF-67p/GCE, Ag-ZIF-67/GCE and Ag-ZIF-67p/GCE (in the presence and absence of DA/AP). Reproduced with permission from ref. 78. Copyright (2020) Elsevier.

An amperometry glucose sensing using ZIF-8 encapsulated TiO_2 platform was prepared.[112] Another electrochemical sensor for glucose detection based on Ag@TiO_2@ ZIF-67 nanocomposite was synthesized.[100] The above two as-synthesized nanocomposites were using ZIFs and TiO_2 for the glucose sensor application. On the other hand, the GOx@ZIF-8(TiO_2)/GCE and Ag@TiO_2@ZIF-67/GCE were both fabricated by the drop-casting method, and the GOx@ZIF-8(TiO_2) composites showed a significantly lower LOD than the Ag@TiO_2@ZIF-67 composites for the detection of glucose (80 nM *vs.* 0.99 μM). One reason to explain this phenomenon: GOx@ZIF-8(TiO_2) composites were synthesized by encapsulating TiO_2 and GOx inside ZIF-8 MOF, an enzymatic sensor, while Ag@TiO_2@ ZIF-67/GCE was a nonenzymatic sensor. The common denominator is that the above two sensors both exhibited extremely sensitive and selective glucose.

Fe_3O_4 was also vital metal oxide that could be combined with ZIFs to form functional nanocomposite materials. It has been reported that the Fe_3O_4@ZIF-8/RGO nanocomposites were made up of Fe_3O_4, ZIF-8, and RGO (reduced graphite oxide) for the detection of DA,[94] while the Fe_3O_4/PPy@ZIF-8 nanocomposites consisted of Fe_3O_4, ZIF-8, and Polypyrrole (PPy) for the detection of glucose.[113] At first, Fe_3O_4 was decorated on RGO, and then ZIF-8 was wrapped on the surface of Fe_3O_4 to obtain the Fe_3O_4@ZIF-8/RGO nanocomposite.[94] However, the Fe_3O_4/PPy@ZIF-8 nanocomposites had a different synthetic route, made PPy polymerization on the surface of Fe_3O_4 to obtain Fe_3O_4/PPy, and ZIF-8 was coated on the PPy to get Fe_3O_4/PPy@ZIF-8 nanocomposite, and then GOx was immobilized

on the Fe_3O_4/PPy@ZIF-8 nanocomposite, as shown in Fig. 12a. Moreover, the size of the two as-prepared nanocomposites was the same, about 200 nm, and their morphology was also remarkable like each other, Fe_3O_4@ZIF-8 and Fe_3O_4/PPy both owned the core–shell structure. Fig. 12b shows the TEM images of Fe_3O_4@ZIF-8, Fe_3O_4/PPy and Fe_3O_4/PPy@ZIF-8. In addition, the Fe_3O_4@ZIF-8/RGO/GCE biosensor owned the best voltammetric response than Fe_3O_4/RGO/GECE and Fe_3O_4@ZIF-8/GCE towards DA detection.[94] At the same time, compared with the Fe_3O_4@ZIF-8/GCE, the Fe_3O_4/PPy@ZIF-8/GCE biosensor also showed a higher anodic peak for the detection of glucose (Fig. 12c). Fig. 12d shows the typical *I–t* curves of GOx/Fe_3O_4/PPy@ZIF-8/GCE towards glucose. The current increased quickly and reached the steady-state current within 5 s for each injection of glucose. The corresponding calibration curves displayed in inset of Fig. 12d suggested the good linear relationship and wide linear range and the detection limit of the biosensor was 0.333 μM based on S/N = 3. Both nanocomposites were prepared using the drop-casting method and were non-enzyme biosensors, and while they were able to detect different small biomolecules, they both displayed exceptional electrochemical performance, including outstanding selectivity, reproducibility, and stability. Furthermore, these nanocomposites were effective in detecting real samples.

5.3 ZIF-derived bimetallic composites

There are very few reports about the ZIF-derived bimetallic composites as electrochemical sensors for the detection of small biomolecules. Two kinds of glucose sensing platforms
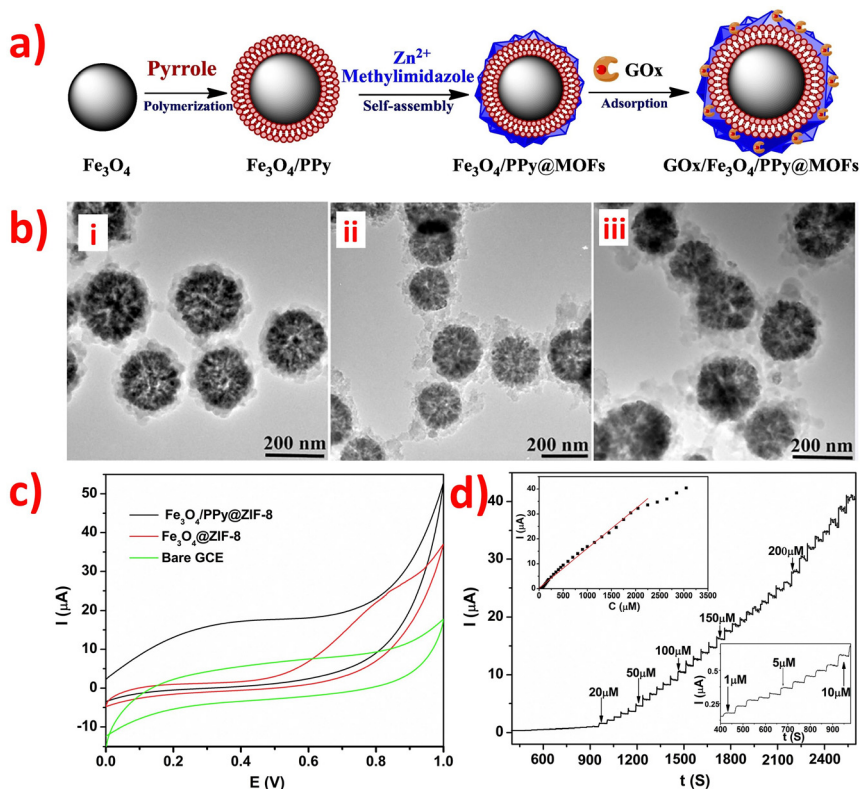
Fig. 12 (a) Scheme for the preparation of Fe$_3$O$_4$/PPy@ZIF-8 nanocomposite and the application of glucose detection. (b) TEM images of the (i) Fe$_3$O$_4$@ZIF-8, (ii) Fe$_3$O$_4$/PPy and (iii) Fe$_3$O$_4$/PPy@ZIF-8. (c) CVs at the bare GCE, the Fe$_3$O$_4$@ZIF-8/GCE, and the Fe$_3$O$_4$/PPy@ZIF-8/GCE in the presence of 0.1 M of H$_2$O$_2$ in PBS (0.1 M, pH 7) at scan rate: 50 mV s^{-1}. (d) I–t response of GOx/Fe$_3$O$_4$/PPy@ZIF-8/GCE to successive addition of glucose in PBS (0.1 M, pH = 7) at applied potential of 0.6 V. Reproduced with permission from ref. 113. Copyright (2018) Elsevier.

have been reported based on ZIFs-derived bimetallic composites: NiCoNSs/GNR/GCE[95] and CoFe-PBA/Co-ZIF/NF.[101] The two composites were prepared through an *in situ* grown strategy, and the sensors were fabricated by the drop-coating method. Among them, the NiCoNSs/GNR/GCE was synthesized by combining ZIF-67-derived bimetallic NiCo layered double hydroxide nanosheets, and graphene nanoribbons (GNRs) fabricated on the surface of GCE, which could increase the electrical conductivity due to the π–π interactions of the final composite modifier film with the GCE. The CoFe-PBA/Co-ZIF/NF was prepared *via* a simple hydrothermal method: a classic two-dimensional (2D) ZIFs (Co-ZIF and Fe-ZIF) were *in situ* converted into PBAs, and then fabricated PBA/ZIF nanocomposites on the surface of nickel foam (NF), which exhibited high electrochemical sensing performance and enhanced electrocatalytic activity due to the using of ZIFs as the sacrificial template and the adding of NF increasing the conductivity and opening active sites. There are many distinct reasons why the above three sensors had different LODs for the detection of glucose (0.6 μM *vs.* 0.02 μM): other bimetallic nanoparticles, using different electrodes, combining different functional groups, and so on. In addition, a novel DA sensor was developed based on the CoP@C/NCS composite,[76] which used P-doped bimetallic ZIF-67@ZIF-8 (ZIF-67@ZIF-8-P) as the precursor, and then the CoP

nanoparticles coated with carbon layers were well-dispersed on N-doped carbon spheres.

6. ZIF-polymer materials for electrochemical detection of small biomolecules

6.1 ZIFs-polymer materials

There have been limited reports on using ZIF-derived polymer materials as electrochemical sensors for detecting small biomolecules. However, the combination of ZIFs and highly conductive polymers can lead to the synthesis of conductive MOFs-based composites, which hold promise as materials for constructing electrochemical sensors A novel electrochemical sensor was developed based on Nafion/polyaniline/ZIF-8, which exhibited high electrochemical performance towards DA oxidation owing to the large surface area of ZIF-8 and the excellent electrical conductivity of polyaniline (PANI).[88] The Nafion/PANI/ZIF-8/GCE was fabricated by electrodeposition of the composite film on the surface of GCE. Additionally, Nafion was used as a cation exchange polymer to improve the selectivity and sensitivity towards DA detection by rejecting negatively charged interferences such as AA. The high electrocatalytic performance of the sensor was attributed to the large surface
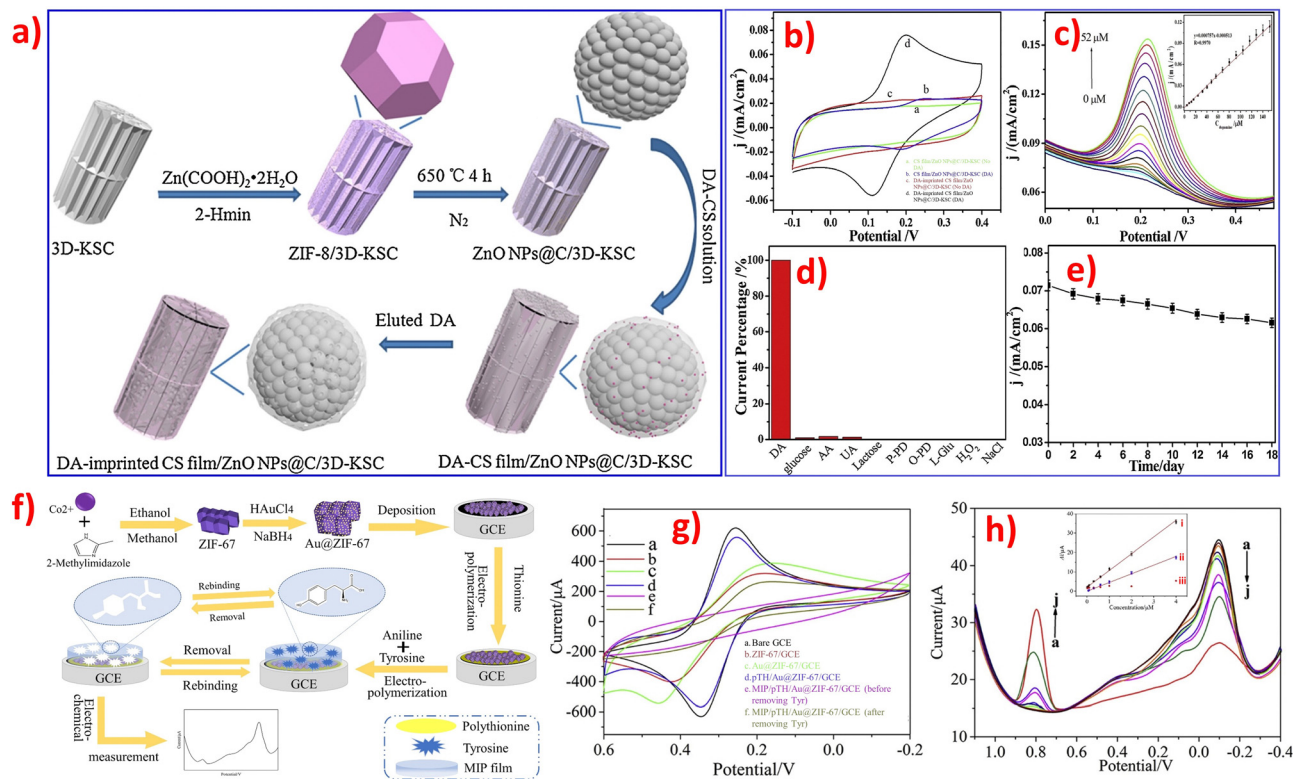
This journal is © The Royal Society of Chemistry 2023

J. Mater. Chem. B, 2023, **11**, 9099–9127 | **9121**

area of ZIF-8 and the excellent electrical conductivity of PANI.[88,142] Furthermore, NF has many advantages, such as chemical and thermal stability, mechanical strength, chemical inertness, good electrical conductivity, and proper adhesion on electrode surfaces. Nafion/PANI/ZIF-8/GCE performed better redox peaks of DA than bare GCE, ZIF-8/GCE, PANI/GCE, and PANI/ZIF-8/GCE, suggesting NF plays a significant role in the electrochemical sensing platform. In addition, the addition of NF polymer could increase the accumulation of the positively charged molecules *via* electrostatic interaction, resulting in enhanced sensitivity of the measurements.[142] A novel electrochemical sensing platform was constructed that consisted of a radiometric electrochemical sensor associated with a self-cleaning electrode, which was based on polydimethylsiloxane (PDMS)@cZIF nanocomposites that were synthesized *via* combining a hydrophobic organic polymer (PDMS) and ZIF.[88] The PDMS@cZIF/GCE was prepared by the drop-coating method, and it exhibited excellent electrocatalytic ability for simultaneous detection of adrenaline, serotonin, and tryptophan. It can be observed that the peak currents of PDMS@cZIF/GCE and cZIF/GCE were higher than bare GCE, ZIF-67@ZIF-8, which could provide a proper redox potential and did not interfere with the electrochemical reactions of others.

6.2 ZIFs and molecular imprinting polymer (MIP)

The preparation of molecularly imprinted polymer (MIP)-based sensors has gained widespread interest in modern analysis technology and has been frequently integrated with electrochemical measurement methods.[13] MIPs offer several advantages, such as specific recognition ability, good stability, low cost, ease of preparation, high selectivity, long service life, and wide application range.[85,132] Despite their advantages, MIPs also have some limitations, such as poor conductivity, a limited number of imprinted cavities, and low sensitivity. However, the integration of MIPs with suitable electrocatalytic nanomaterials can lead to the development of sensors with improved electrochemical performance, addressing these issues. Several MIP-based sensors have been reported to exhibit superior performance compared to traditional electrochemical sensors in detecting target molecules, thanks to their exceptional selectivity and strong affinity. For example, it has been reported that there were three kinds of MIP-based electrochemical sensing for the detection of DA: MIPs/CuCo$_2$O$_4$@carbon/3D-KSC/IE,[75] DA-imprinted CS film/ZnONPs@C/3D-KSC/IE,[74] and PPy/ZIF-67-MIPs/Nafion/GCE.[85] Among them, the MIPs/CuCo$_2$O$_4$@ carbon/3D-KSC/IE and the DA-imprinted CS film/ZnO NPs@ C/3D-KSC/IE were prepared *via* electrodepositing method fabricated by an integrated electrode (IE), while the PPy/ZIF-67 MIPs/Nafion/GCE was prepared by the drop-coating method fabricated on the surface of GCE. A simple and effective MIP-based sensor was developed using a PPy/ZIF-67 MIPs/Nafion hybrid. The sensor utilized a conductive PPy film with high conductivity, excellent selectivity, and good biocompatibility. Additionally, Nafion was added to the sensor to improve dispersion performance. ZIF-67 was synthesized using a simple hydrothermal method and subsequently subjected to an oxidation reaction using FeCl$_3$ solution to obtain a black suspension in the same container. At last, the ultrasonicated suspension was used to modify the surface of the GCE, followed by the fabrication of an electrochemical device using continuous CV technique to remove DA. The synergistic effect of ZIF-67, PPy, and Nafion in the MIP-based sensor led to improved adsorption and determination of DA. However, the preparation of MIPs/CuCo$_2$O$_4$@carbon/3D-KSC/IE was slightly complex. At first, calcined the ZIF-derived bimetallic nanocomposites (CuCo-ZIF) and arrayed them on 3D-KSCs to obtain the CuCo$_2$O$_4$@carbon/3D-KSCs. Secondly, used chitosan (CS) as MIPs to form a DA-CS polymer film and electrodeposited it on the surface of CuCo$_2$O$_4$@ carbon/3D-KSC to develop a MIPs/ CuCo$_2$O$_4$@carbon/3D-KSC integrated electrode for the detection of DA. As shown in Fig. 13a, the preparation of the DA-imprinted chitosan (CS) film/ZnO nanoparticles (NPs)@carbon(C)/three-dimensional kenaf stem-derived microporous carbon (3D-KSC) integrated electrode was quite complicated, which was prepared by growing ZIF-8 on 3D-KSC and carbonizing under high temperature and anaerobic condition to obtain porous ZnONPs@C nanosphere/3D-KSC, and then electrodepositing the DA-CS on the surface of the nMIP/ZnONPs@C/3D-KSC integrated electrode to form the final product of DA-imprinted CS film/ZnO NPs@C/3D-KSC integrated electrode for the detection of DA.[74] Both DA sensors mentioned above utilized chitosan (CS) as the functional polymer matrix for the MIPs and employed porous 3D-KSCs as the supporting base materials. Different ZIFs materials were allowed to grow on the surface of the 3D-KSCs to obtain various composites by carbonizing. The final MIP-based sensors were then formed by a simple electrodeposition method on the surface of the integrated electrodes. Under optimized conditions, the electrochemical performance of CS film/ZnO NPs@C/3D-KSC and DA-imprinted CS film/ZnO NPs@C/3D-KSC (Fig. 13b) were explored to demonstrate that the DA-imprinted CS film had a strong rebinding ability to DA. Although the current density response of ZnO NPs@C/3D-KSC toward DA was larger than that of DA-imprinted CS film/ZnO NPs@C/3D-KSC, its selectivity was poor. Moreover, the DA-imprinted CS film/ZnO NPs@C/3D-KSC integrated electrode had a significantly lower LOD (Fig. 13c) than the MIPs/CuCo$_2$O$_4$@carbon/3D-KSC integrated electrode (0.039 nM *vs.* 0.16 μM), suggesting ZnO NPs are a good promising candidate that combinate with 3D-KSC to construct the electrochemical sensors. DA-imprinted CS film/ZnO NPs@C/3D-KSC also depicted a good repeatability and good stability (Fig. 13d and e). In addition, the use of MIPs could improve selectivity and sensitivity due to their unique recognition property toward DA. A complex AA-imprinted MIP sensor has been reported, which was synthesized firstly by growing ZIF-67 on carbon cloth (CC) to obtain ZIF-67/CC as a working electrode, and then AA-imprinted ploy(o-PD) was successively deposited through electropolymerization on the surface of ZIF-67/CC electrode.[132] At last, the AA-poly(o-PD)/ZIF-67CC was placed in a mixture of K Cl and ethanol to remove AA to obtain MIPs/ZIF-67/CC electrode. Moreover, the MIPs/ZIF-67/CC electrode exhibited superior

9122 | *J. Mater. Chem. B*, 2023, **11**, 9099–9127

This journal is © The Royal Society of Chemistry 2023

Fig. 13   (a) Schematic illustrating preparation of DA-imprinted CS film/ZnO NPs@C/3D-KSC. (b) CVs of CS film/ZnO NPs@C/3D-KSC and DA-imprinted CS film/ZnO NPs@C/3D-KSC in 0.2 M PBS (pH = 7.0) without DA and with 0.10 mM DA. (c) DPV of DA-imprinted CS film/ZnO NPs@C/3D-KSC in 0.2 M PBS (pH = 7.0) with different concentrations of DA. Inset: Calibration curve. (d) The current response of DA-imprinted CS film/ZnO NPs@C/3D-KSC in 0.2 M PBS (pH = 7.0) with some substances. (e) The repeatability of DA-imprinted CS film/ZnO NPs@C/3D-KSC in detecting 0.10 mM DA in 0.2 M PBS (pH = 7.0). Reproduced with permission from ref. 74. Copyright (2019) Elsevier. (f) Illustration of the MIP/pTH/Au@ZIF-67/GCE fabrication and electro-chemical measurement process. (g) CV curves of different electrodes in 5 mM [Fe(CN)$_6$]$^{3-/4-}$ containing 0.1 M KCl. (h) DPVs of the MIP/pTH/Au@ZIF-67/GCE sensor toward various concentrations of Tyr in 0.1 M PBS (pH = 5.0). Inset: Calibration plot between Tyr concentration and dual-signal current changes ($\Delta i = |\Delta i_{Tyr}| + |\Delta i_{TH}|$) with (i) MIP/pTH/Au@ZIF-67/GCE and (iii) NIP/pTH/Au@ZIF-67/GCE, and (ii) the calibration plot between Tyr concentration and single-signal current changes of Tyr (Δi_{Tyr}). Reproduced with permission from ref. 13. Copyright (2020) Elsevier.

performance to CC, ZIF-67/CC, and NIPs/ZIF-67/CC. In addition, it has been reported another complex MIP-based dual-signal electrochemical sensor that was used for the detection of tyrosine: MIP/pTH/Au@ZIF-67/GCE.[13] The synthesis step and the detection principle of the tyrosine-imprinted MIP sensor were familiar with the AA-imprinted MIP sensor. The MIP/pTH/Au@ZIF-67 composites were prepared as follows: synthesized Au@ZIF-67 composites and modified them on the surface of a bare GCE, then the Poly thionine was deposited on the Au@ZIF-67/GCE surface by electropolymerization method (Fig. 13f). This MIP was prepared *via* the CVs technique, and the tyrosine template molecules were eluted from the porous MIP membrane to carry out electron transport to generate an electrochemical signal for the detection of tyrosine. It is worth noting that this sensing system is based on a dual-signal strategy with DPV peak currents ($\Delta i = |\Delta i_{Tyr}| + |i_{TH}|$, $|\Delta i_{Tyr}|$ is the current intensity increase of Tyr and $|i_{TH}|$ is the peak current decrease of pTH), which showed satisfied electrochemical performance (Fig. 13h). Moreover, compared with the MIP/pTH/Au@ZIF-67/GCE, the peak current of NIP (non-imprinted polymer)/pTH/Au@ZIF-67/GCE

was not obvious, suggesting the poor conductivity of polyaniline film and the importance of MIPs (Fig. 13g).

7. Conclusions and outlook for the future

In recent years, there has been a growing trend of using electrochemical sensors based on ZIFs materials or their derivatives modified by different electrodes for the detection of small biomolecules in human body fluids, owing to their unique structures and excellent electrocatalytic performance. Despite this progress, finding suitable sensitive and selective sensors based on ZIFs remains a considerable challenge for many scientists in the fields of biological, medical, and environmental research. Although a few reports have utilized ZIFs for the simultaneous determination of multiple small biomolecules, there have only been a handful of sensors based on ZIFs for detecting amino acids and adrenaline, with most studies focusing on the detection of DA or glucose. Furthermore, some sensors have exhibited excellent electrochemical

performance, with an exceptionally LOD of approximately 0.1 μM or even less than 0.1 μM. In addition, these working electrodes based on ZIFs materials have been efficiently used for the analysis of small biomolecules in real samples such as human urine, amino acid injection, and human serum, and have achieved satisfactory results. Furthermore, the nano-particles or functional groups of these ZIFs or ZIFs-derived composites can provide large surface areas, excellent conductivity, and many catalytically active sites, thereby enhancing the sensing capabilities of these materials.

In this review, we have summarized various composites of ZIFs with other materials, such as carbon-based materials, metal or metal oxide-based materials, polymer materials, and ZIFs-derived materials, for the detection of different small biomolecules. Among these composites, various carbon materials were used most frequently, with graphene materials being particularly popular and attracting a lot of interest from researchers. The combination of unconventional materials with ZIFs or ZIFs derivatives to form composites could exhibit more advantages than using the individual materials alone, high-lighting the importance of synergistic effects. Furthermore, while most studies focused on ZIF-8 (Zn-based) or ZIF-67 (Co-based) materials, it will be a new challenge for researchers to explore other ZIFs and their derivatives in the future. Most ZIF-derived materials have been used for the detection of glucose, but it is crucial for scientists to develop new and effective ZIF-derived materials to detect other small biomolecules such as DA, UA, and AA. There are many advantages of using ZIFs or ZIFs-derived composites as promising candidates for electro-chemical sensing. Firstly, ZIFs belong to a subclass of MOFs that typically exhibit stable morphology, porous or microporous structures, and excellent physicochemical performance. Sec-ondly, compared to other MOFs that may require the use of organic solvents, most ZIFs can be synthesized using water as a solvent at room temperature, making them more environmen-tally and economically friendly. Lastly, ZIF-67 is known to form hollow or porous structures of Co_3O_4-carbon nanowires, which can provide high stability for immobilizing enzymes such as GOx, resulting in better detection sensitivity. However, despite the development of electrochemical sensors based on ZIFs materials, many problems and limitations still need to be urgently addressed based on existing reports in the electroche-mical field. For example, in most papers, the electrocatalytic mechanism of some small biomolecules was not reported, or only the possible electrocatalytic mechanism (such as glucose) was reported without certainty of its accuracy. Moreover, these ZIFs or ZIFs-derived composites can be influenced by many factors, such as morphology, topography, chemical composi-tion, active area, crystallographic texture, and conductivity. It is not yet clear which of these factors may have the most sig-nificant impact on the catalytic activity of the entire sensing device, and further research is needed to fully understand the underlying mechanisms. Furthermore, it has been shown that the electrochemical procedure of DA is an adsorption-controlled process on the electrode surface, but the charge distribution and mass of DA and dopaminophenone inside the

composites are still uncertain. However, with the incorporation of graphene materials, the resulting composites can form attractive π–π interactions with analytes, leading to an increase in catalytic activity for electron transfer towards DA. However, the exact role of ZIFs in these mechanisms remains unclear. Additionally, some ZIF-based composites may be unstable in aqueous solutions, which can cause the collapse of the crystal structure of the composites and detachment from the surface of the electrode. Most ZIF-derived materials use ZIF-67 as the precursor and template, resulting in hollow core–shell nanos-tructures. Although ZIF-8 has a similar structure and organic ligands to ZIF-67, there is a lack of comparison experiments using ZIF-8 as the precursor and template. Some MIP-based sensors show better selectivity for analysis than other tradi-tional sensors, but many reports do not provide information on their specific reaction mechanism. Lastly, there are very few studies involving density functional theory calculations and molecular dynamics simulations, which could potentially explain structure-performance relationships and reaction mechanisms.

In summary, ZIFs or ZIFs-derived materials have numerous advantages and great potential in electrocatalysis. However, there are still many challenges in the detection of various small biomolecules, and scientists will face more difficulties in practical applications, mass production, and cost savings. Looking ahead, there is a promising outlook for the develop-ment of environmentally friendly composites and their applica-tion in various fields. With the advancement of electrochemical techniques, more biomolecules or essential compounds can be analyzed using ZIF-based electrochemical sensing devices. Finally, a critical challenge for scientists is to develop ZIFs or ZIFs-derived materials that can be applied to the rapid and simultaneous detection of multiple biomolecules.

Conflicts of interest

The authors declare that they have no known competing fiscal interests or personal relationships that could have appeared to influence the work reported in this paper.

Acknowledgements

References

1 Z. Qiu, T. Yang, R. Gao, G. Jie and W. Hou, *J. Electroanal. Chem.*, 2019, **835**, 123–129.

2 B. Ma, H. Guo, M. Wang, L. Li, X. Jia, H. Chen, R. Xue and W. Yang, *Electroanalysis*, 2019, **31**, 1002–1008.

3 Y. Wang, H. Ge, G. Ye, H. Chen and X. Hu, *J. Mater. Chem. B*, 2015, **3**, 3747–3753.

9124 | *J. Mater. Chem. B*, 2023, **11**, 9099–9127

This journal is © The Royal Society of Chemistry 2023

4 H. Duan, Z. Zhao, J. Lu, W. Hu, Y. Zhang, S. Li, M. Zhang, R. Zhu and H. Pang, *ACS Appl. Mater. Interfaces*, 2021, **13**, 33083–33090.

5 K. Jayaramulu, M. Horn, A. Schneemann, H. Saini, A. Bakandritsos, V. Ranc, M. Petr, V. Stavila, C. Narayana and B. Scheibe, *Adv. Mater.*, 2021, **33**, 2004560.

6 N. Setoudeh, S. Jahani, M. Kazemipour, M. M. Foroughi and H. H. Nadiki, *J. Electroanal. Chem.*, 2020, **863**, 114045.

7 W. Yang, X. Shi, Y. Li and H. Pang, *J. Energy Storage*, 2019, **26**, 101018.

8 G. Zhao, T. Wang, L. Li, Y. Tang, Q. Qin and C. Wu, *Carbon*, 2021, **183**, 291–300.

9 P. Kukkar, K. H. Kim, D. Kukkar and P. Singh, *Coord. Chem. Rev.*, 2021, **446**, 214109.

10 J. Zhang, Y. Tan and W. J. Song, *Microchim. Acta*, 2020, **187**, 1–23.

11 H. N. Abdelhamid, *Biointerface Res. Appl. Chem.*, 2021, **11**, 8283–8297.

12 Y. R. Lee, M. S. Jang, H. Y. Cho, H. J. Kwon, S. Kim and W. S. Ahn, *Chem. Eng. J.*, 2015, **271**, 276–280.

13 B. Chen, Y. Zhang, L. Lin, H. Chen and M. Zhao, *J. Electroanal. Chem.*, 2020, **863**, 114052.

14 C. H. Voon and S. T. Sam, *Nanobiosensors for Biomolecular Targeting*, Elsevier, 2019, pp. 23–50.

15 J. Kumar, L. K. Narnoliya and A. Alok, *Current developments in biotechnology and bioengineering*, Elsevier, 2019, pp. 143–161.

16 B. Hu, Y. Liu, Z. W. Wang, Y. Song, M. Wang, Z. Zhang and C. S. Liu, *Appl. Surf. Sci.*, 2018, **441**, 694–707.

17 S. Lan, Y. Song, Q. Chen, Z. Guo and H. Zhan, *Electrochim. Acta*, 2016, **217**, 47–54.

18 S. Baluchová, A. Daňhel, H. Dejmková, V. Ostatná, M. Fojta and K. Schwarzová-Pecková, *Anal. Chim. Acta*, 2019, **1077**, 30–66.

19 Z. H. Sheng, X. Q. Zheng, J. Y. Xu, W. J. Bao, F. B. Wang and X. H. Xia, *Biosens. Bioelectron.*, 2012, **34**, 125–131.

20 D. Han, T. Han, C. Shan, A. Ivaska and L. J. E. Niu, *Electroanalysis*, 2010, **22**, 2001–2008.

21 Y. Li, X. J. S. Lin and A. B. Chemical, *Sens. Actuators, B*, 2006, **115**, 134–139.

22 J. Ping, J. Wu, Y. Wang and Y. Ying, *Biosens. Bioelectron.*, 2012, **34**, 70–76.

23 A. Savk, B. Özdil, B. Demirkan, M. S. Nas, M. H. Calimli, M. H. Alma, A. M. Asiri and F. Şen, *Mater. Sci. Eng., C*, 2019, **99**, 248–254.

24 M. A. Kachouei, S. Shahrokhian and M. Ezzati, *Sens. Actuators, B*, 2021, **344**, 130254.

25 Y. Zhao, S. Zhao, J. Huang and F. Ye, *Talanta*, 2011, **85**, 2650–2654.

26 W. Pormsila, S. Krähenbühl and P. C. Hauser, *Anal. Chim. Acta*, 2009, **636**, 224–228.

27 B. M. Costa, A. A. Prado, T. C. Oliveira, L. P. Bressan, R. A. Munoz, A. D. Batista, J. A. da Silva and E. M. Richter, *Talanta*, 2019, **204**, 353–358.

28 X. Wang, Y. Zhang, C. Cheng, R. Dong and J. Hao, *Analyst*, 2011, **136**, 1753–1759.

29 J. Chen, Y. P. Shi and J. Y. Liu, *J. Chromatogr. A*, 2003, **1003**, 127–132.

30 J. Zhao, *Biomed. Chromatogr.*, 2015, **29**, 410–415.

31 J. Lykkesfeldt, *Anal. Biochem.*, 2000, **282**, 89–93.

32 C. Ma, Z. Sun, C. Chen, L. Zhang and S. Zhu, *Food Chem.*, 2014, **145**, 784–788.

33 H. Y. Wang, Y. Sun and B. Tang, *Talanta*, 2002, **57**, 899–907.

34 N. E. Azmi, N. I. Ramli, J. Abdullah, M. A. A. Hamid, H. Sidek, S. Abd Rahman, N. Ariffin and N. A. Yusof, *Biosens. Bioelectron.*, 2015, **67**, 129–133.

35 X. Wu, Y. Diao, C. Sun, J. Yang, Y. Wang and S. Sun, *Talanta*, 2003, **59**, 95–99.

36 J. F. Sierra, J. Galban, S. De Marcos and J. R. Castillo, *Anal. Chim. Acta*, 2000, **414**, 33–41.

37 S. L. Grant, Y. Shulman, P. Tibbo, D. R. Hampson and G. B. Baker, *J. Chromatogr. B*, 2006, **844**, 278–282.

38 Å. Bertler, A. Carlsson and E. Rosengren, *Acta Physiol. Scand.*, 1958, **44**, 273–292.

39 L. Zhang, N. Teshima, T. Hasebe, M. Kurihara and T. Kawashima, *Talanta*, 1999, **50**, 677–683.

40 R. D. Chaudhari, A. B. Joshi and R. Srivastava, *Sens. Actuators, B*, 2012, **173**, 882–889.

41 H. Chen, Q. Wang, Q. Shen, X. Liu, W. Li, Z. Nie and S. Yao, *Biosens. Bioelectron.*, 2017, **91**, 878–884.

42 G. J. Zhou, G. F. Zhang and H. Y. Chen, *Anal. Chim. Acta*, 2002, **463**, 257–263.

43 H. Li, C. Liu, D. Wang and C. Zhang, *Biosens. Bioelectron.*, 2017, **91**, 268–275.

44 J. W. Costin, P. S. Francis and S. W. Lewis, *Anal. Chim. Acta*, 2003, **480**, 67–77.

45 D. Wen, W. Liu, A. K. Herrmann, D. Haubold, M. Holzschuh, F. Simon and A. Eychmüller, *Small*, 2016, **12**, 2439–2442.

46 X. Wang, F. Li, Z. Cai, K. Liu, J. Li, B. Zhang and J. He, *Anal. Bioanal. Chem.*, 2018, **410**, 2647–2655.

47 J. Peng, J. Ling, X. Q. Zhang, L. Y. Zhang, Q. E. Cao and Z. T. Ding, *Sens. Actuators, B*, 2015, **221**, 708–716.

48 H. Rosen, *Arch. Biochem. Biophys.*, 1957, **67**, 10–15.

49 Z. Chen, Y. Hu, Q. Yang, C. Wan, Y. Tan and H. Ma, *Sens. Actuators, B*, 2015, **207**, 277–280.

50 A. Weißenstein, C. R. Saha-Möller and F. Würthner, *Chem. – Eur. J.*, 2018, **24**, 8009–8016.

51 P. A. Rasheed and J. S. Lee, *Microchim. Acta*, 2017, **184**, 1239–1266.

52 J. Wang, Y. Chang, W. B. Wu, P. Zhang, S. Q. Lie and C. Z. Huang, *Talanta*, 2016, **152**, 314–320.

53 H. W. Park, S. M. Alam, S. H. Lee, M. M. Karim, S. M. Wabaidur, M. Kang and J. H. Choi, *Luminescence*, 2009, **24**, 367–371.

54 J. Huang, H. Fang, C. Liu, E. Gu and D. Jiang, *Anal. Lett.*, 2008, **41**, 1430–1442.

55 J. R. Lakowicz and B. Maliwal, *Anal. Chim. Acta*, 1993, **271**, 155–164.

56 D. S. Kim, E. S. Kang, S. Baek, S. S. Choo, Y. H. Chung, D. Lee, J. Min and T. H. Kim, *Sci. Rep.*, 2018, **8**, 14049.

This journal is © The Royal Society of Chemistry 2023

J. Mater. Chem. B, 2023, **11**, 9099–9127 | **9125**

57 S. Liu, X. Xing, J. Yu, W. Lian, J. Li, M. Cui and J. Huang, *Biosens. Bioelectron.*, 2012, **36**, 186–191.

58 S. I. Kaya, S. Kurbanoglu and S. A. Ozkan, *Crit. Rev. Anal. Chem.*, 2019, **49**, 101–125.

59 G. Luo, Y. Deng, X. Zhang, R. Zou, W. Sun, B. Li, B. Sun, Y. Wang and G. Li, *New J. Chem.*, 2019, **43**, 16819–16828.

60 S. Pramanik, Y. Kumar, D. Gupta, V. K. Vashistha, A. Kumar, P. Karmakar and D. K. Das, *Mater. Sci. Eng., B*, 2021, **272**, 115356.

61 C. Missale, S. R. Nash, S. W. Robinson, M. Jaber and M. G. Caron, *Physiol. Rev.*, 1998, **78**, 189–225.

62 L. Yang, D. Liu, J. Huang and T. You, *Sens. Actuators, B*, 2014, **193**, 166–172.

63 I. Stone, *Orthomol. Psychiatry*, 1972, **1**, 82–89.

64 S. Chambial, S. Dwivedi, K. K. Shukla, P. J. John and P. Sharma, *Indian J. Clin. Biochem.*, 2013, **28**, 314–328.

65 R. J. Jariwalla and S. Harakeh, *Subcell. Biochem.*, 1996, 215–231.

66 D. R. Gallie, *Scientifica*, 2013, **2013**, 795964.

67 M. Yu, K. Zhao, X. Zhu, S. Tang, Z. Nie, Y. Huang, P. Zhao and S. Yao, *Biosens. Bioelectron.*, 2017, **95**, 41–47.

68 Z. Yang, J. J. C. You, S. A. Physicochemical and E. Aspects, *Colloids Surf., A*, 2021, **612**, 126064.

69 Y. Zhang, Y. Q. Liu, Y. Bai, X. Li and W. Chu, *Appl. Surf. Sci.*, 2021, **539**, 148235.

70 S. M. Babulal, S.-M. Chen, R. Palani, K. Venkatesh, A. S. Haidyrah, S. K. Ramaraj, C. C. Yang and C. Karuppiah, *Colloids Surf., A*, 2021, **621**, 126600.

71 K. Massey, C. Blakeslee and H. Pitkow, *Amino Acids*, 1998, **14**, 271–300.

72 G. Wu, Z. Wu, Z. Dai, Y. Yang, W. Wang, C. Liu, B. Wang, J. Wang and Y. Yin, *Amino Acids*, 2013, **44**, 1107–1113.

73 K. Manjunatha, B. K. Swamy, H. Madhuchandra and K. Vishnumurthy, *Chem. Data Collect.*, 2021, **31**, 100604.

74 Y. Song, J. Han, L. Xu, L. Miao, C. Peng and L. Wang, *Sens. Actuators, B*, 2019, **298**, 126949.

75 L. Wang, H. Yang, L. Xu, C. Peng and Y. Song, *J. Alloys Compd.*, 2020, **817**, 152771.

76 L. Xiao, S. Zheng, K. Yang, J. Duan and J. Jiang, *Microchem. J.*, 2021, **168**, 106432.

77 T. Fan, L. Chen, S. Qiu, C. Yang, L. Hu, X. Peng, J. Zhang and Z. Yan, *J. Electroanal. Chem.*, 2020, **878**, 114541.

78 J. Tang, Y. Liu, J. Hu, S. Zheng, X. Wang, H. Zhou and B. Jin, *Microchem. J.*, 2020, **155**, 104759.

79 Y. Dong and J. Zheng, *Sens. Actuators, B*, 2020, **311**, 127918.

80 S. Lu, M. Hummel, K. Chen, Y. Zhou, S. Kang and Z. Gu, *Electrochem. Commun.*, 2020, **114**, 106715.

81 W. Yao, H. Guo, H. Liu, Q. Li, N. Wu, L. Li, M. Wang, T. Fan and W. Yang, *Microchem. J.*, 2020, **152**, 104357.

82 N. T. T. Tu, P. C. Sy, T. V. Thien, T. T. T. Toan, N. H. Phong, H. T. Long and D. Q. Khieu, *J. Mater. Sci.*, 2019, **54**, 11654–11670.

83 W. Chen, D. Ji, Y. Zhang, P. Xu, X. Gao, J. Fang, X. Li, L. Feng and W. Wen, *Nanotechnology*, 2019, **30**, 335708.

84 Q. Xu, R. Qiu, H. Jiang and X. Wang, *J. Electroanal. Chem.*, 2019, **839**, 247–255.

85 W. Zhang, D. Duan, S. Liu, Y. Zhang, L. Leng, X. Li, N. Chen and Y. Zhang, *Biosens. Bioelectron.*, 2018, **118**, 129–136.

86 J. Tang, S. Jiang, Y. Liu, S. Zheng, L. Bai, J. Guo and J. Wang, *Microchim. Acta*, 2018, **185**, 1–11.

87 C. Srinivas, M. Sudharsan, G. R. K. Reddy, P. S. Kumar, A. J. Amali and D. Suresh, *Electroanalysis*, 2018, **30**, 2475–2482.

88 Y. Yuan, J. Xia, F. Zhang, Z. Wang and Q. Liu, *J. Electroanal. Chem.*, 2018, **824**, 147–152.

89 H. Guo, M. Wang, L. Zhao, N. Youliwasi and C. Liu, *Microporous Mesoporous Mater.*, 2018, **263**, 21–27.

90 G. Yu, J. Xia, F. Zhang and Z. Wang, *J. Electroanal. Chem.*, 2017, **801**, 496–502.

91 P. Xu, M. Liu, X. Li, T. Xu and Y. Zhang, 2017.

92 M. Nie, S. Lu, D. Lei, C. Yang and Z. Zhao, *J. Electrochem. Soc.*, 2017, **164**, H952.

93 Y. Y. Zheng, C. X. Li, X. T. Ding, Q. Yang, Y. M. Qi, H. M. Zhang and L. T. Qu, *Chin. Chem. Lett.*, 2017, **28**, 1473–1478.

94 Y. Wang, Y. Zhang, C. Hou and M. Liu, *RSC Adv.*, 2015, **5**, 98260–98268.

95 P. Gai, H. Zhang, Y. Zhang, W. Liu, G. Zhu, X. Zhang and J. Chen, *J. Mater. Chem. B*, 2013, **1**, 2742–2749.

96 E. Asadian, S. Shahrokhian and A. I. Zad, *J. Electroanal. Chem.*, 2018, **808**, 114–123.

97 R. Singh, M. Musameh, Y. Gao, B. Ozcelik, X. Mulet and C. M. Doherty, *J. Mater. Chem. C*, 2021, **9**, 7677–7688.

98 G. Mo, X. Zheng, N. Ye and Z. Ruan, *Talanta*, 2021, **225**, 121954.

99 Z. Zhao, Y. Sun, Y. Huang, J. Jin, X. Wei, W. Gong, J. Hu and Y. Chen, *Microchem. J.*, 2021, **160**, 105623.

100 D. Arif, Z. Hussain, M. Sohail, M. A. Liaqat, M. A. Khan and T. Noor, *Front. Chem.*, 2020, **8**, 573510.

101 C. Chen, D. Xiong, M. Gu, C. Lu, F.-Y. Yi and X. Ma, *ACS Appl. Mater. Interfaces*, 2020, **12**, 35365–35374.

102 Q. Zhu, S. Hu, L. Zhang, Y. Li, C. Carraro, R. Maboudian, W. Wei, A. Liu, Y. Zhang and S. Liu, *Sens. Actuators, B*, 2020, **313**, 128031.

103 Q. Guo, W. Zeng, S. Liu and Y. Li, *Nanotechnology*, 2020, **31**, 265501.

104 Y. Feng, D. Xiang, Y. Qiu, L. Li, Y. Li, K. Wu and L. Zhu, *Electroanalysis*, 2020, **32**, 571–580.

105 Y. Qin, Y. Sun, Y. Li, C. Li, L. Wang and S. Guo, *Chin. Chem. Lett.*, 2020, **31**, 774–778.

106 C. Hou, X. Zhang, L. Wang, F. Zhang, X. Huang and Z. Wang, *Microchim. Acta*, 2020, **187**, 1–8.

107 L. Wang, X. Miao, Y. Qu, C. Duan, B. Wang, Q. Yu, J. Gao, D. Song, Y. Li and Z. Yin, *J. Electroanal. Chem.*, 2020, **858**, 113810.

108 C. Chen, Y. Zhong, S. Cheng, Y. Huanga, T. Li, T. Shi, G. Liao and Z. Tang, *J. Electrochem. Soc.*, 2020, **167**, 027531.

109 L. Xiao, Q. Zhao, L. Jia, Q. Chen, J. Jiang and Q. Yu, *Electrochim. Acta*, 2019, **304**, 456–464.

110 Y. Zhang, Y. Zhang, H. Zhu, S. Li, C. Jiang, R. J. Blue and Y. Su, *J. Alloys Compd.*, 2019, **780**, 98–106.

111 X. Chen, D. Liu, G. Cao, Y. Tang and C. Wu, *ACS Appl. Mater. Interfaces*, 2019, **11**, 9374–9384.

112 A. Paul and D. N. Srivastava, *ACS Omega*, 2018, **3**, 14634–14640.

113 C. Hou, D. Zhao, Y. Wang, S. Zhang and S. Li, *J. Electroanal. Chem.*, 2018, **822**, 50–56.

114 A. Paul, G. Vyas, P. Paul and D. N. Srivastava, *ACS Appl. Nano Mater.*, 2018, **1**, 3600–3607.

115 P. Sukhrobov, S. Numonov, X. Mamat, Y. Li, T. Wågberg and G. Hu, *Int. J. Electrochem. Sci.*, 2018, **13**, 6550–6564.

116 W. Meng, Y. Wen, L. Dai, Z. He and L. Wang, *Sens. Actuators, B*, 2018, **260**, 852–860.

117 C. Xiong, T. Zhang, W. Kong, Z. Zhang, H. Qu, W. Chen, Y. Wang, L. Luo and L. Zheng, *Biosens. Bioelectron.*, 2018, **101**, 21–28.

118 L. Shi, X. Cai, H. Li, H. He, H. Zhao and M. Lan, *Electroanalysis*, 2018, **30**, 466–473.

119 B. Xue, K. Li, L. Feng, J. Lu and L. Zhang, *Electrochim. Acta*, 2017, **239**, 36–44.

120 E. Zhang, Y. Xie, S. Ci, J. Jia and Z. Wen, *Biosens. Bioelectron.*, 2016, **81**, 46–53.

121 L. Shi, X. Zhu, T. Liu, H. Zhao and M. Lan, *Sens. Actuators, B*, 2016, **227**, 583–590.

122 Y. Wang, C. Hou, Y. Zhang, F. He, M. Liu and X. Li, *J. Mater. Chem. B*, 2016, **4**, 3695–3702.

123 Elizbit, U. Liaqat, Z. Hussain, M. M. Baig, M. A. Khan and D. Arif, *J. Korean Ceram. Soc.*, 2021, **58**, 598–605.

124 Q. Sun, J. Ding, D. Chen, C. Han, M. Jiang, T. T. Li, Y. Hu, J. Qian and S. Huang, *ChemElectroChem*, 2021, **8**, 812–818.

125 Q. Chen, D. Chu, L. Yan, H. Lai, X.-Q. Chu, D. Ge and X. Chen, *New J. Chem.*, 2021, **45**, 10031–10039.

126 T. S. Thanh, P. T. Qui, N. T. T. Tu, T. T. T. Toan, T. T. B. Hoa, L. V. T. Son, D. M. Nguyen, T. N. Tuyen and D. Q. Khieu, *J. Nanomater.*, 2021, **2021**, 1–13.

127 K. Wang, C. Wu, F. Wang, M. Liao and G. Jiang, *Biosens. Bioelectron.*, 2020, **150**, 111869.

128 H. T. Ngo, L. T. Hoa, N. T. Khanh, T. T. B. Hoa, T. T. T. Toan, T. X. Mau, N. H. Phong, H. S. Thang and D. Q. Khieu, *J. Nanomater.*, 2020, **2020**, 1–13.

129 L. Liu, L. Liu, Y. Wang and B. C. Ye, *Talanta*, 2019, **199**, 478–484.

130 J. Xu, J. Xia, F. Zhang and Z. Wang, *Electrochim. Acta*, 2017, **251**, 71–80.

131 Y. Ma, Y. Zhang and L. Wang, *Talanta*, 2021, **226**, 122105.

132 Y. Guo, L. Wang, L. Xu, C. Peng and Y. Song, *J. Mater. Sci.*, 2020, **55**, 9425–9435.

133 Y. Li, W. Ye, Y. Cui, B. Li, Y. Yang and G. Qian, *J. Mol. Struct.*, 2020, **1209**, 127986.

134 G. Pan, Y. Song, L. Miao and L. Wang, *Ionics*, 2017, **23**, 2377–2385.

135 J. Zhang, D. Wang and Y. Li, *ACS Appl. Mater. Interfaces*, 2019, **11**, 13557–13563.

136 X. Cai, Y. Mo, Z. Ruan and G. Mo, *J. Colloid Interface Sci.*, 2021, **603**, 822–833.

137 J. Zeng, R. Xu, L. Jiao, Y. Wang, L. Chen, C. D. Windle, X. Ding, Z. Zhang, Q. Han and L. Qu, *J. Mater. Chem. B*, 2019, **7**, 5291–5295.

138 A. Phan, C. J. Doonan, F. J. Uribe-Romo, C. B. Knobler, M. O'keeffe and O. M. Yaghi, 2009.

139 J. Qian, F. Sun and L. Qin, *Mater. Lett.*, 2012, **82**, 220–223.

140 A. K. S. Kumar, Y. Zhang, D. Li and R. G. Compton, *Electrochem. Commun.*, 2020, **121**, 106867.

141 L.-L. Gao and E.-Q. Gao, *Coord. Chem. Rev.*, 2021, **434**, 213784.

142 N. F. Atta, A. Galal and D. M. El-Said, *ACS Omega*, 2019, **4**, 17947–17955.

143 F. Nasirpouri, K. Alipour, F. Daneshvar and M.-R. Sanaeian, *Corrosion Protection at the Nanoscale*, Elsevier, 2020, pp. 473–497.

144 A. Abbaspour, A. Khajehzadeh and A. Ghaffarinejad, *Analyst*, 2009, **134**, 1692–1698.

145 T. Yoshitake, J. Kehr, K. Todoroki, H. Nohta and M. Yamaguchi, *Biomed. Chromatogr.*, 2006, **20**, 267–281.

146 S. Marinesco and N. Dale, *Microelectrode Biosensors*, Springer, 2013.

147 N. P. Shetti, D. S. Nayak, K. R. Reddy and T. M. Aminabhvi, *Graphene-based electrochemical sensors for biomolecules*, Elsevier, 2019, pp. 235–274.

148 Y. A. Yarkaeva, D. Dubrovskii, R. Zil'berg and V. Maistrenko, *Russ. J. Electrochem.*, 2020, **56**, 544–555.

149 A. Safavi, N. Maleki, O. Moradlou and F. Tajabadi, *Anal. Biochem.*, 2006, **359**, 224–229.

150 R. J. Mortimer, 1999.

151 A. Amine and H. Mohammadi, *Ref. Modul. Chem. Mol. Sci. Chem. Eng.*, 2018, 70–79, DOI: 10.1016/B978-0-12-409547-2.14204-0.

152 S. Baluta, F. Meloni, K. Halicka, A. Szyszka, A. Zucca, M. I. Pilo and J. Cabaj, *RSC Adv.*, 2022, **12**, 25342–25353.

153 P. Dauphin-Ducharme, N. Arroyo-Currás, M. Kurnik, G. Ortega, H. Li and K. W. Plaxco, *Langmuir*, 2017, **33**, 4407–4413.

154 R. Seeber and F. Terzi, *J. Solid State Electrochem.*, 2011, **15**, 1523–1534.

155 A. Pellicano, 2015.

156 J. R. Castle and W. K. Ward, *J. Diabetes Sci. Technol.*, 2010, **4**, 221–225.

157 A. C. Marques, T. Pinheiro, G. V. Martins, A. R. Cardoso, R. Martins, M. G. Sales and E. Fortunato, *Comprehensive Analytical Chemistry*, Elsevier, 2020, vol. 89, pp. 189–237.

158 H. Karimi-Maleh, Y. Orooji, F. Karimi, M. Alizadeh, M. Baghayeri, J. Rouhi, S. Tajik, H. Beitollahi, S. Agarwal and V. K. Gupta, *Biosens. Bioelectron.*, 2021, **184**, 113252.

159 M. Sajid, M. K. Nazal, M. Mansha, A. Alsharaa, S. M. S. Jillani and C. Basheer, *TrAC, Trends Anal. Chem.*, 2016, **76**, 15–29.

160 S. Abu Nayem, S. Shaheen Shah, N. Sultana, M. A. Aziz and A. Saleh Ahammad, *Chem. Record*, 2021, **21**, 1039–1072.

161 K. Scida, P. W. Stege, G. Haby, G. A. Messina and C. D. García, *Anal. Chim. Acta*, 2011, **691**, 6–17.

162 S. Wang, B. Ye, C. An, X. Song and J. Wang, *J. Mater. Sci.*, 2020, **55**, 4646–4655.

163 H. Liu, T. Xu, C. Cai, K. Liu, W. Liu, M. Zhang, H. Du, C. Si and K. Zhang, *Adv. Funct. Mater.*, 2022, **32**, 2113082.

This journal is © The Royal Society of Chemistry 2023

J. Mater. Chem. B, 2023, **11**, 9099–9127 | 9127